


ORIGINAL RESEARCH

# *Panax notoginseng* Saponin Protects Against Diabetic Cardiomyopathy Through Lipid Metabolism Modulation

Chenyang Zhang, PhD; Bin Zhang, PhD; Xuelian Zhang, PhD; Min Wang, PhD; Xiaobo Sun , PhD; Guibo Sun, PhD

**BACKGROUND:** People with diabetes are more likely to develop cardiovascular diseases. Lipotoxicity plays a key role in the development of diabetic cardiomyopathy. *Panax notoginseng* saponin (PNS) has been used to treat diabetes and obesity. However, the role of PNS in diabetic cardiomyopathy remains unclear.

**METHODS AND RESULTS:** Diabetic db/db mice received high-dose (200 mg/kg per day) or medium-dose (100 mg/kg per day) PNS by gavage for 12 weeks until week 36. Lipid accumulation and cardiac function in diabetic mice were detected and possible mechanisms involved were explored. PNS significantly improved body weight, body fat content, serum lipids, adipocytokines, and antioxidative function in db/db mice. Lipid accumulation in adipose tissue, liver, and heart were also alleviated by PNS treatment. Cardiac function and mitochondrial structure were also improved by PNS. H9c2 cells were treated with palmitate acid, and PNS pretreatment reduced lipid accumulation, mitochondrial reactive oxygen species, as well as improved mitochondrial membrane potential and mitochondrial oxygen consumption rate. Levels of proteins and expression of genes related to glucose and lipid metabolism, antioxidative function, and mitochondrial dynamics were also improved by PNS administration.

**CONCLUSIONS:** PNS attenuated heart dysfunction in diabetic mice by reducing lipotoxicity as well as modulating oxidative stress and improving mitochondrial function.

**Key Words:** diabetic cardiomyopathy ■ lipid metabolism ■ mitochondria ■ oxidative stress ■ PNS

Although the cause of type 2 diabetes is multifactorial, obesity has been proven to play a critical role in its progression.<sup>1</sup> It has been shown that type 2 diabetes is accompanied by excessive fat accumulation in the liver, which worsens hepatic responsiveness to insulin, resulting in increased glucose production.<sup>2</sup> In addition, adipose tissue is also responsible for multiorgan insulin resistance through elevated levels of circulatory factors such as free fatty acids (FFAs) and leptin, which promote hyperglycemia.<sup>3</sup> Diabetes has become an epidemic in recent years, and cardiovascular complications are the major cause of death in people with diabetes.<sup>4</sup> People

with diabetes are more likely to develop cardiovascular complications and have a poorer prognosis than those without diabetes.<sup>4</sup> Diabetic cardiomyopathy is a condition resulting from diabetes in which heart failure occurs without coronary artery disease, hypertension, or valvular heart disease.<sup>5</sup> Many potential mechanisms have been recommended, such as mitochondrial dysfunction, increased lipid use, excessive reactive oxygen species (ROS) production, and lipotoxicity, but the exact mechanism remains relatively underinvestigated and requires further study. Aminoguanidine breakers,<sup>6</sup> metformin,<sup>7</sup> angiotensin-converting enzyme inhibitors,<sup>8</sup> beta blockers (timolol),<sup>9</sup> and dipeptidyl peptidase-4

Correspondence to: Xiaobo Sun, PhD, and Guibo Sun, PhD, Institute of Medicinal Plant Development, Peking Union Medical College and Chinese Academy of Medical Sciences, No.151 Malianwa North Road, Haidian District, Beijing 100193, P. R. China. E-mail: sun\_xiaobo163@163.com, sunguibo@126.com  
Supplemental Material for this article is available at <https://www.ahajournals.org/doi/suppl/10.1161/JAHA.121.023540>

For Sources of Funding and Disclosures, see page 18.

© 2022 The Authors. Published on behalf of the American Heart Association, Inc., by Wiley. This is an open access article under the terms of the Creative Commons Attribution-NonCommercial-NoDerivs License, which permits use and distribution in any medium, provided the original work is properly cited, the use is non-commercial and no modifications or adaptations are made.

JAHA is available at: [www.ahajournals.org/journal/jaha](http://www.ahajournals.org/journal/jaha)

## CLINICAL PERSPECTIVE

### What Is New?

- *Panax notoginseng* saponin (PNS) treatment significantly improved body weight, body fat content, serum lipids, adipocytokines, and antioxidative function in diabetic mice. Lipid accumulation in adipose tissue, liver, and heart was also alleviated by PNS treatment.
- PNS alleviated heart failure and mitochondrial dysfunction by modulating lipid metabolism, improving antioxidative function and mitochondrial dynamics.

### What Are the Clinical Implications?

- PNS can alleviate obesity and reduce lipid accumulation in diverse organs as well as improve function of adipose tissue, liver, and heart.
- PNS can attenuate heart failure caused by diabetes by reducing lipotoxicity as well as modulating oxidative stress and improving mitochondrial function.

## Nonstandard Abbreviations and Acronyms

<b>FS</b>	fractional shortening
<b>LVAW</b>	left ventricular anterior wall thickness
<b>LVID</b>	left ventricular internal diameter
<b>NRF</b>	nuclear respiratory factor
<b>PNS</b>	<i>Panax notoginseng</i> saponin
<b>SOD</b>	superoxide dismutase

inhibitors,<sup>10</sup> as well as other putative therapies such as sodium-glucose transport protein 2 inhibitors and glucagon-like peptide 1 agonists, have exerted beneficial effects on diabetic cardiomyopathy in preclinical animal models. However, none of these therapies has been used clinically to treat patients with diabetic cardiomyopathy.<sup>11</sup> Therefore, there is an urgent need to further elucidate the mechanisms of and find new therapies targeting diabetic cardiomyopathy.

Recently, traditional Chinese medicine has increased in popularity. *Panax notoginseng* has been used to manage bleeding in China for thousands of years. *Panax notoginseng* saponin (PNS) is the main active ingredient in *Panax notoginseng* and the main ingredient of Xuesaitong injection. Many experiments have demonstrated that PNS can protect against cardiovascular diseases, probably owing to antiplatelet, anticoagulant, antithrombotic, antiatherosclerotic, and lipid-lowering effects and so on.<sup>12</sup> PNS has also been reported to treat diabetes and obesity in KK-Ay

mice.<sup>13,14</sup> Moreover, PNS can protect against endoplasmic reticulum stress and oxidative stress in cardiomyocytes,<sup>15,16</sup> improve myocardial energy metabolism, rescue myocardial damage, and inhibit ischemia-induced apoptosis of cardiomyocytes.<sup>17–19</sup> Additionally, PNS can protect against acute myocardial infarction and heart failure by inducing autophagy.<sup>20</sup> All these experiments demonstrated that PNS exerted beneficial effects on cardiac protection. However, none of these studies has focused on the role of PNS in diabetic cardiomyopathy.

This study demonstrated the basic mechanisms of the later stages of diabetic cardiomyopathy and the protective effects of PNS on diabetic cardiomyopathy. By week 36, the control diabetic mice showed elevated body weight and fat level, increased levels of serum lipids, and lipid accumulation in the liver and adipose tissue, and PNS administration reduced lipid accumulation in diabetic mice of the test group. Furthermore, diabetic mice experienced severe heart failure with obvious cardiac hypertrophy, fibrosis, and apoptosis in the diabetic heart. Excessive lipid accumulation in the diabetic heart, which is the primary feature of diabetic cardiomyopathy, was the main cause of ROS production. Excess ROS accumulation in the mitochondria was also detected, which is one of the reasons for mitochondrial dysfunction. Destroyed mitochondrial function and morphology were observed, which may have led to reduced energy supply and finally caused heart failure. However, PNS treatment significantly reduced lipid accumulation, decreased ROS production, and repaired mitochondrial function, which improved cardiac structure and function in diabetic mice. These findings suggest that PNS protects against diabetic cardiomyopathy by reducing lipid accumulation as well as modulating antioxidant status and promoting mitochondrial energy supply to inhibit heart failure.

## METHODS

The data that support the findings of this study are available from the corresponding author upon reasonable request.

### Materials

PNS came from Kunming Shenghuo Pharmaceutical Co., Ltd and metformin was obtained from Sino American Shanghai Squibb Pharmaceutical Co., Ltd. Study design of this research and quality control of PNS used in this research were listed in Figure 1. Antibodies used in this research were all obtained from Abclonal Technology (Wuhan, China).

### Experimental Animals

All experiments were carried out according to the recommended guidelines and approved by the Laboratory

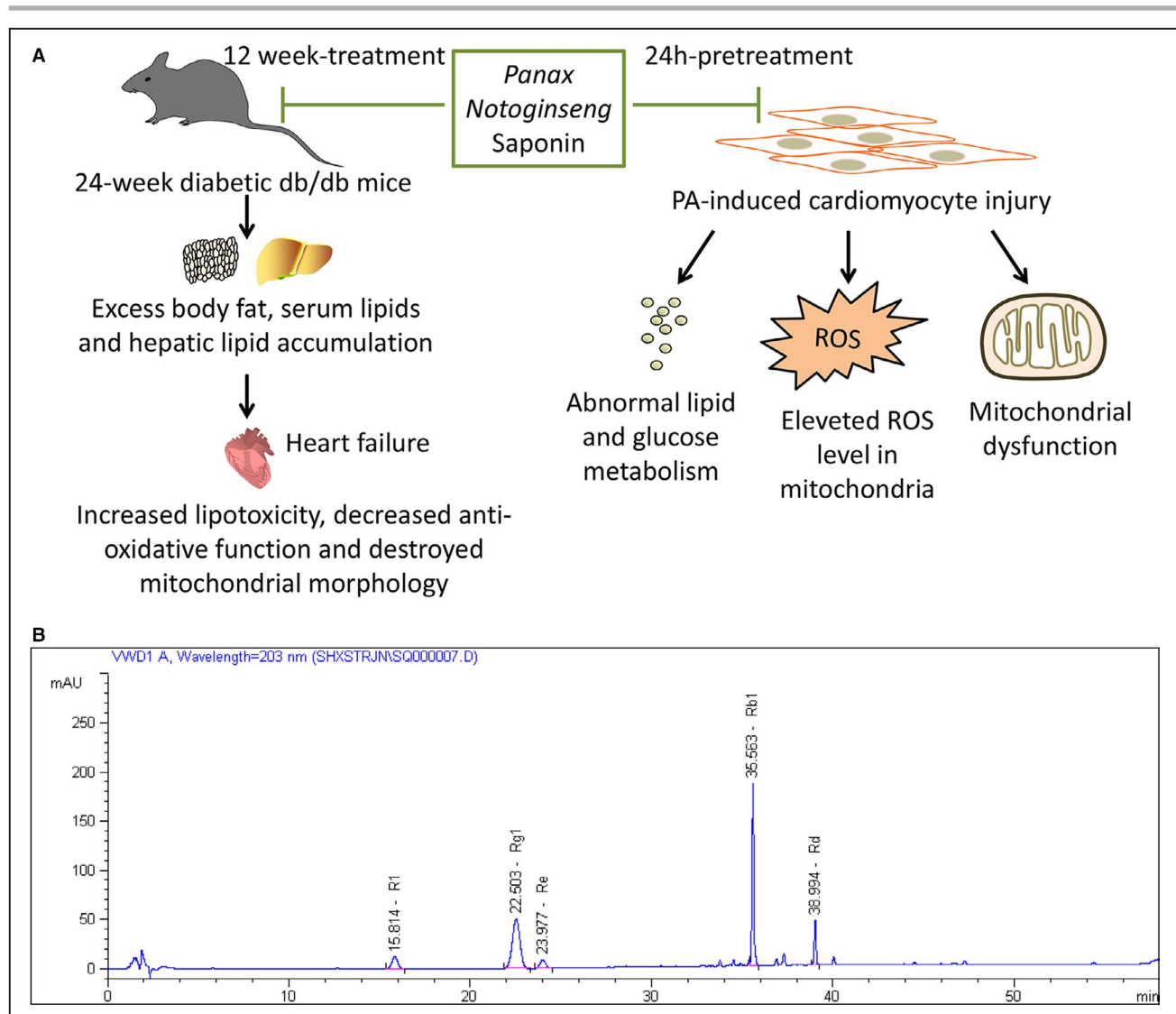


**Figure 1. Study design and PNS quality control.**

**A**, Study design of this research: diabetic db/db mice were gavaged with *Panax notoginseng* saponin, after 12-week treatment, body weight, body fat, blood glucose and serum lipids, adipokines, and biochemical indexes related to antioxidative stress and inflammation were detected. Cardiac function, pathological change, and mitochondrial structure were also investigated. H9c2 cells were treated with palmitate acid and after PNS pretreatment, lipid accumulation, mitochondrial reactive oxygen species, mitochondrial membrane potential, and mitochondrial oxygen consumption rate were detected. Levels of proteins and expression of genes related to glucose and lipid metabolism, antioxidative function, and mitochondrial dynamics were also investigated. **B**, HPLC analysis of PNS used in this research. PNS used for gavage met the quality control requirements of the Chinese Pharmacopoeia, which stated that the content of notoginsenoside R1, ginsenoside Rg1, ginsenoside Re, ginsenoside Rb1, and ginsenoside Rd in PNS were no <5%, 25%, 2.5%, 30%, and 5%, respectively. In addition, total content of notoginsenoside R1, ginsenoside Rg1, ginsenoside Re, ginsenoside Rb1, and ginsenoside Rd in PNS was no <75%. Each retention time of peak in HPLC of PNS was in accordance with its standard control. HPLC indicates high-performance liquid chromatography; PA, palmitate acid; PNS, *Panax notoginseng* saponin; and ROS, reactive oxygen species.

Animal Ethics Committee of the Institute of Medicinal Plant Development, Peking Union Medical College. Eight-week-old male db/m and db/db mice were purchased from Vital River Laboratory Animal Technology Co., Ltd. (Beijing, China). Female mice were not chosen because estrogen may have protective effect in diabetic cardiomyopathy. All animals were kept in a thermostatic room with a 12-hour light-dark cycle and had free access to

food and water until 24 weeks old. All animals were randomized into 5 groups: (1) db/m group (Control), (2) db/db group (Model), (3) db/db+metformin 250 mg/kg per day group (metformin), (4) db/db+PNS 200 mg/kg per day group (H-PNS), and (5) db/db+PNS 100 mg/kg per day group (M-PNS). PNS or metformin was administered to the mice every day for 12 weeks. Mice in the control and model groups were administered pure water.

## Blood Tests

Fasting blood glucose levels in overnight-fasted mice were measured after 12 weeks of treatment using the blood collected from the tail vein. Blood samples were collected from retro-orbital sinus of mice after anesthesia, kept at room temperature for 2 hours, centrifuged at 3000×g for 15 minutes, and then harvested for further analyses. Lipid content, including contents of total triglyceride (TG), total cholesterol, high-density lipoprotein, low-density lipoprotein, and FFAs, as well as levels of liver function markers including alanine aminotransferase and aspartate aminotransferase were measured using an automatic biochemical analyzer (AU480, Beckman Coulter, USA). Serum creatine kinase (CK), creatine kinase-MB (CK-MB), and lactate dehydrogenase (LDH) levels were measured using a fully automatic biochemical analyzer (AU480, Beckman Coulter). Catalase, malondialdehyde, superoxide dismutase (SOD), and glutathione (GSH) peroxidase assay kits (Nanjing Jianchen Bioengineering Institute, China) were used to detect serum lipid peroxidation according to the manufacturer's instructions. Insulin, adiponectin, and leptin levels, as well as levels of proinflammatory cytokines such as interleukin-6 (IL-6), interleukin 1 $\alpha$  (IL-1 $\alpha$ ), MCP-1 (monocyte chemoattractant protein-1), tumor necrosis factor- $\alpha$ , and CRP (C-reactive protein), were quantified using kits according to the manufacturer's instructions (Beijing Huaying Institute of Biological Technology, China).

## Echocardiography

After 12 weeks of treatment, echocardiography was performed using the Vevo 770 Imaging System (VisualSonics, Canada), and each parameter was measured twice. All the mice were anesthetized using isoflurane (RDW, China). Echocardiographic parameters were detected in the parasternal long-axis view. Left ventricular internal diameter (LVID), left ventricular anterior wall thickness (LVAW), and left ventricular posterior wall thickness (LVPW) were measured. Left ventricular volume (LV vol), left ventricular ejection fraction (EF), and fractional shortening (FS) were calculated.

## Histology and Transmission Electron Microscopy

Whole mouse hearts were fixed in formalin and embedded in paraffin for histological analysis. After being cut into 5  $\mu$ m sections and stained with hematoxylin and eosin (HE), Masson's trichrome, Oil Red O, and TdT-mediated dUTP nick-end labeling (TUNEL), images from left ventricle of each heart were acquired with a panoramic scanning microscope (3DHISTECH, Hungary) and processed using Caseviewer version 2.4 (3DHISTECH). For transmission electron microscopic analysis, left ventricle of each mouse heart was fixed with 2.5% glutaraldehyde

(Sigma, USA). Mitochondrial ultrastructure in the heart sections was observed using a Tecnai G2 Spirit transmission electron microscope (Thermo Fisher, USA). Liver and subcutaneous adipose tissues of mice were stained with HE, and livers were also stained with Oil Red O after fixation and embedding.

## Cell Culture and Treatment

Rat embryonic cardiac myoblasts (H9c2) were purchased from the Cell Bank of the Chinese Academy of Sciences (Shanghai, China). DMEM supplemented with 10% fetal bovine serum was used to grow cells at 37 °C under 5% CO<sub>2</sub> atmosphere. When cells reached about 80% confluency, they were pretreated with different concentrations of PNS or 5  $\mu$ mol/L berberine for 24 hours and then incubated in fetal bovine serum-free DMEM with or without palmitate acid (PA) for 24 hours. The 3T3-L1 mouse preadipocytes were purchased and maintained in the same atmosphere as that of H9c2. Two days after the cells were confluent, differentiation was induced by exposure to 1  $\mu$ mol/L dexamethasone, 0.5 mmol/L 3-isobutyl-1-methylxanthine, and 10  $\mu$ g/mL insulin in DMEM with 10% fetal bovine serum for 48 hours. Two days later, the medium was changed to differentiation medium (10  $\mu$ g/mL insulin in DMEM with 10% fetal bovine serum). After 48 hours of treatment, the medium was replaced. The cells were then used in the experiments.

## Cell Viability

Cell viability was assessed using 3-(4,5-dimethylthiazol-2-yl)-2,5-diphenyltetrazolium bromide (Solarbio, China). After seeding in 96-well plates and reaching 80% confluency, cells were treated with different concentrations of PNS or PA. They were then incubated with 1 mg/mL 5-diphenyltetrazolium bromide for 4 hours at 37 °C without light. At the end of the incubation, the medium was aspirated, dimethyl sulfoxide was added, and the absorbance was measured using a microplate reader at OD 570 nm.

## BODIPY Staining

BODIPY 493/503 was used to measure intracellular lipid accumulation in H9c2 and 3T3-L1 cells (Invitrogen, USA). After fixing with 4% paraformaldehyde, the cells were washed 3 times and incubated with the BODIPY working solution at room temperature in the dark for 30 minutes. After incubation, the cells were washed 3 times with PBS for subsequent fluorescence microscopy imaging (Olympus, Japan).

## Superoxide Measurement

Mitochondrial ROS were measured using MitoSOX Red (Invitrogen). After washing 3 times with PBS, H9c2

cells were incubated with MitoSOX Red working solution at 37 °C without light for 20 minutes. The cells were then washed 3 times with PBS before mitochondrial ROS imaging using a fluorescence microscope (Olympus).

### Measurement of GSH:Oxidized Glutathione

H9c2 cells were seeded in 6-well plates and after treated with 100 µg/mL PNS for 24 hours followed by 300 µmol/L PA treatment, cells were washed with PBS and harvested for measurement of GSH:oxidized glutathione according to the kit's instructions (Beyotime, China).

### Measurement of Mitochondrion Membrane Potential ( $\Delta\Psi$ m)

Changes in  $\Delta\Psi$  m were measured using JC-1 staining (Thermo Fisher Scientific). H9c2 cells were seeded in 6-well plates, and after the cells reached about 80% confluence, they were treated with 100 µg/mL PNS or 50 µg/mL PNS for 24 hours, followed by the addition of 300 µmol/L PA. After 24 hours, the medium was discarded, and 2 µg/mL JC-1 was added and incubated at 37 °C for 20 minutes, and the cells were washed with PBS and photographed using a fluorescence microscope (Olympus).

### Mitochondrial Staining

Mitochondria were stained as follows: The cells were plated in 6-well plates. After PNS and PA treatment, the cells were washed with PBS 3 times and then stained for 30 minutes at 37 °C with MitoTracker Red and Hoechst 33342 (Invitrogen). The cells were then washed with PBS, and mitochondria were imaged using a fluorescence microscope (Olympus).

### Measurement of Mitochondrial Oxygen Consumption Rate

To record the oxygen consumption rate of H9c2 cells, an XF24 extracellular flux analyzer was used according to the manufacturer's instructions (Agilent Seahorse Bioscience, USA). Cells were seeded in an Agilent Seahorse XF24 Cell Culture Microplate (Agilent Seahorse Bioscience). After PNS and PA treatment, oxygen consumption rate was recorded following the experimental tips, and basal and maximal oxygen consumption rates were calculated and normalized with cell counts.

### Quantitative Reverse-Transcription Polymerase Chain Reaction

Total mRNA was isolated from mouse hearts using TRIzol according to the manufacturer's instructions

(Invitrogen). The quality and quantity of isolated RNA were assessed using Nanodrop 2000 (Thermo Fisher Scientific). Samples with 260/280 and 260/230 ratios between 1.8 and 2.0 were reverse-transcribed into cDNA using the PrimeScript RT Reagent Kit (Takara, Japan). TB Green II (Takara) was used to quantify the polymerase chain reaction-amplified products. The expression levels were calculated using the  $\Delta\Delta C_t$  method. The primer pairs used are listed in Table S1.

### Western Blot Analysis

Samples were fragmented and lysed in lysis buffer at 4 °C for 30 minutes (CW BIO, China). After centrifugation at 12 000×g at 4 °C for 30 minutes, the supernatants were collected, followed by quantification of sample protein concentrations using a BCA Protein Quantitative Assay Kit (CW BIO). Following mixing with loading buffer and boiling for denaturation, protein mixtures were loaded into each well and separated on an 8% sodium dodecyl sulfate-polyacrylamide gel electrophoresis gel. Proteins were then transferred onto nitrocellulose membranes and blocked for 2 hours. After incubation with rabbit polyclonal antibodies against proteins related to mitochondrial dynamics and lipid metabolism at 1:1000 dilution at 4 °C overnight, the membranes were washed with tris-buffered saline with Tween 3 times and incubated with the secondary antibody for 90 minutes, followed by washing with tris-buffered saline with Tween 3 times. Protein bands were detected with ECL Western blot detection kits (CW BIO), and their levels were quantified using ImageJ. All experiments were performed at least 3 times, and the averages were used for comparisons.

### Statistical Analysis

All statistical analyses were performed using the SPSS version 17.0. Data are presented as the mean±SEM. One-way analysis of variance and least significant difference test were used to compare multiple groups. Statistical significance was set at  $P<0.05$ .

## RESULTS

### PNS Reduced Insulin Resistance and Serum Lipid Levels in db/db Mice

As shown in Figure 2A and 2B, at 36 weeks, db/db mice showed significantly increased body weight and blood glucose level compared with that of the controls ( $P<0.01$ ), whereas metformin, a drug long used to control blood glucose level in diabetes, significantly decreased their body weight and glucose levels ( $P<0.05$ ). Both H-PNS and M-PNS improved the body weight ( $P<0.05$ ) rather than blood glucose of diabetic mice ( $P>0.05$ ). Elevated body fat as well as serum insulin and

FFA levels were observed in db/db mice (Figures 2C through 2E,  $P < 0.01$ ), whereas metformin only decreased their body fat level ( $P < 0.05$ ), and both H-PNS and M-PNS treatments improved the 3 elevated levels of diabetic mice ( $P < 0.05$ ). Only H-PNS significantly decreased serum total cholesterol, TG, high-density lipoprotein, and low-density lipoprotein levels in db/db mice (Figure 2F through 2I,  $P < 0.05$ ), treatment with metformin decreased TG and low-density lipoprotein ( $P < 0.05$ ), and M-PNS treatment only decreased low-density lipoprotein ( $P < 0.01$ ). Together, these results indicate that PNS alleviated insulin resistance mainly by reducing lipid levels rather than decreasing blood glucose levels in diabetic mice.

### PNS Reduced Lipid Accumulation in Adipocytes and Improved Inflammation

The extent of fat accumulation in the subcutaneous adipose tissue was evaluated using HE staining. As shown in Figure 3A and 3B, the mean area of adipocytes in the same field of view markedly increased in db/db mice ( $P < 0.001$ ). Metformin and PNS supplementation markedly reduced the mean area of adipocytes ( $P < 0.001$ ), which indicated decreased lipid accumulation in diabetic mice. The 3T3-L1 preadipocytes were also incubated with berberine and PNS to confirm this result. Berberine was used as a positive control according to reports that berberine has a significant effect on lipid reduction.<sup>21</sup> The 5-diphenyltetrazolium

bromide assay was performed to ensure that the PNS concentration used in the experiments was nontoxic (Figure 3C,  $P > 0.05$ ). Subsequently, 50  $\mu\text{g}/\text{mL}$  PNS (M-PNS) and 100  $\mu\text{g}/\text{mL}$  PNS (H-PNS) were used for further research. BODIPY staining on day 4 of differentiation showed significantly decreased lipid accumulation in berberine and PNS-treated mature adipocytes (Figure 3D and 3E,  $P < 0.001$ ), which confirmed that berberine and PNS improved lipid accumulation in adipocytes. PNS treatment also decreased the elevated leptin level (Figure 3F,  $P < 0.01$ ) and increased adiponectin levels in diabetic mice (Figure 3G,  $P < 0.001$ ), which indicated alleviated obesity and insulin resistance in treated mice, whereas metformin only improved adiponectin levels in diabetic mice ( $P < 0.001$ ). Moreover, treatment with PNS significantly improved the inflammation in db/db mice. Serum CRP, tumor necrosis factor- $\alpha$ , MCP1, IL-1 $\beta$ , and IL-6 levels were significantly improved by PNS treatment in db/db mice (Figures 3H through 3L,  $P < 0.01$ ). However, metformin treatment only improved MCP1 levels ( $P < 0.01$ ) and IL-6 levels in diabetic mice ( $P < 0.001$ ). Thus, PNS treatment significantly improved obesity, insulin resistance, and inflammation in diabetic mice.

### PNS Alleviated Fat Accumulation in the Liver and Improved Hepatic Function

HE staining was performed to determine the effects of PNS on morphological and histological changes in

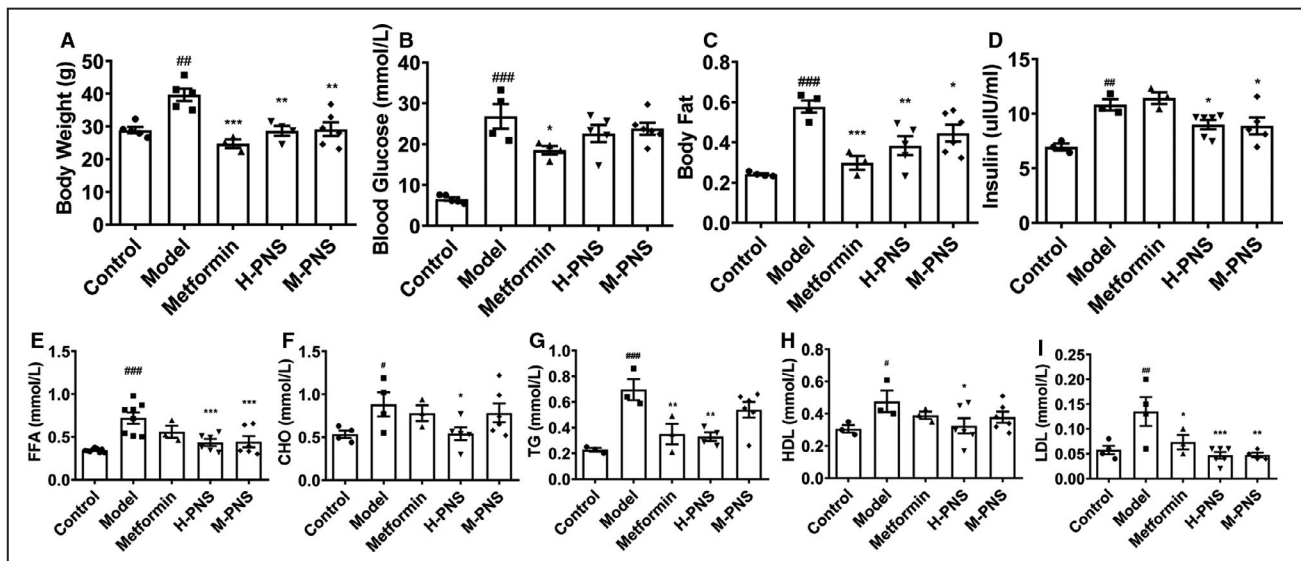


**Figure 2.** PNS reduced lipid accumulation in diabetic mice.

**A**, body weight; **(B)** blood glucose level, and **(C)** body fat level of 36-week-old mice after 12 weeks of treatment. Data are expressed as the mean  $\pm$  SEM ( $n=3-6$ ).  $*P < 0.05$  or  $**P < 0.01$  or  $***P < 0.001$  vs model group;  $\#P < 0.01$  or  $\#\#P < 0.001$  vs the control. Serum **(D)** insulin; **(E)** FFA; **(F)** CHO; **(G)** TG; **(H)** HDL, and **(I)** LDL levels in indicated groups. Data are expressed as the mean  $\pm$  SEM ( $n=3-6$ ).  $*P < 0.05$  or  $**P < 0.01$  or  $***P < 0.001$  vs model group;  $\#P < 0.05$  or  $\#\#P < 0.01$  or  $\#\#\#P < 0.001$  vs the control. CHO indicates total cholesterol; FFA, free fatty acids; HDL, high-density lipoprotein; H-PNS, db/db+PNS 200 mg/kg per day group; LDL, low-density lipoprotein; M-PNS, db/db+PNS 100 mg/kg per day group; PNS, *Panax notoginseng* saponin; and TG, total triglyceride.

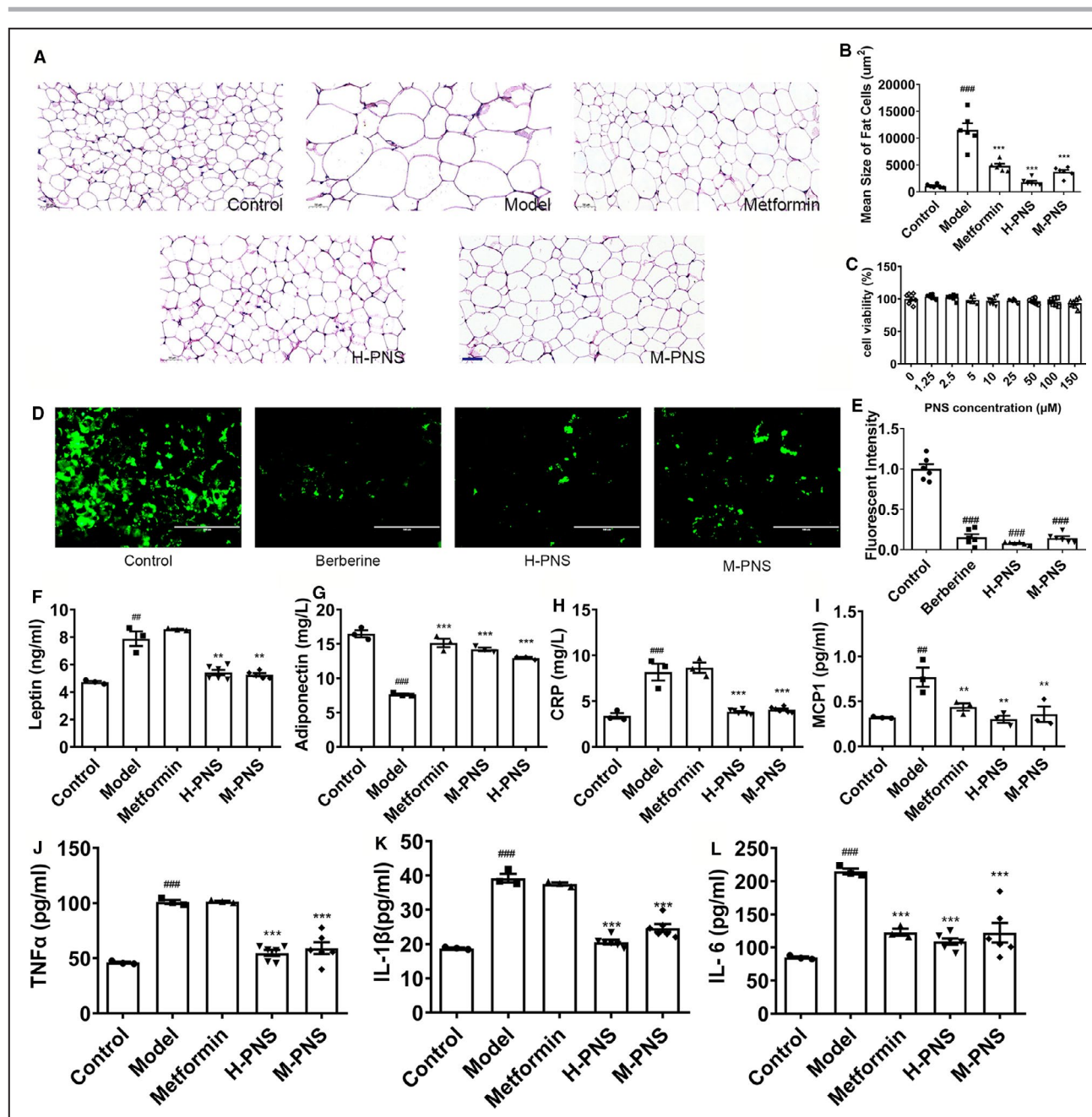


**Figure 3. PNS reduced lipid accumulation and inflammation in adipose tissue.**

**A**, Representative images of HE staining of adipose tissue and **(B)** quantification of adipocyte area. Scale bar, 50 µm. Data are expressed as the mean±SEM (n=6). \*\*\* $P$ <0.001 vs model group; ### $P$ <0.001 vs the control. **C**, MTT assay showing 3T3-L1 cell viability treated using different concentrations of PNS. Data are expressed as the mean±SEM (n=6). **D**, BODIPY staining images showing lipid accumulation in 3T3-L1 cells and **(E)** quantification of green fluorescence in different groups. Scale bar, 200 µm. Data are expressed as the mean±SEM (n=6) ### $P$ <0.001 vs the control. **(F)** leptin; **(G)** adiponectin; **(H)** CRP; **(I)** MCP1; **(J)** TNF-α; **(K)** IL-1β, and **(L)** IL-6 levels in sera of different groups. Data are expressed as the mean±SEM (n=3–6). \* $P$ <0.05 or \*\* $P$ <0.01 or \*\*\* $P$ <0.001 vs model group; ## $P$ <0.01 or ### $P$ <0.001 vs the control. CRP indicates C-reactive protein; HE, hematoxylin and eosin; H-PNS, db/db+PNS 200 mg/kg per day group; IL-1α, interleukin 1α; IL-1β, interleukin-1β; IL-6, interleukin- 6; MCP-1, monocyte chemoattractant protein-1; M-PNS, db/db+PNS 100 mg/kg per day group; MTT, 5-diphenyltetrazolium bromide; PNS, *Panax notoginseng* saponin; and TNF-α, tumor necrosis factor-α.

the liver. Diabetic mice showed enlarged and vacuolar liver cells, whereas metformin and PNS treatments obviously improved the morphology of the liver cells in

the model group (Figure 4A). Consistently, the livers of diabetic mice exhibited increased lipid accumulation compared with that of the control group (Figure 4B

and 4C,  $P < 0.001$ ), whereas metformin and PNS treatments notably reduced lipid droplets in the liver of db/db mice ( $P < 0.001$ ). Moreover, levels of alanine aminotransferase and aspartate aminotransferase, which reflect liver dysfunction, also significantly decreased in metformin or PNS-treated db/db mice (Figure 4D and 4E,  $P < 0.05$ ).

## PNS Improved Cardiac Function in Diabetic Cardiomyopathy

Representative echocardiographic images of the 5 groups are shown in Figure 5A. Representative parameters such as LVID, LVPW, and LVAW were measured; LV volume in diastolic end, EF, and FS were calculated. LVID in diastolic and systolic end significantly increased

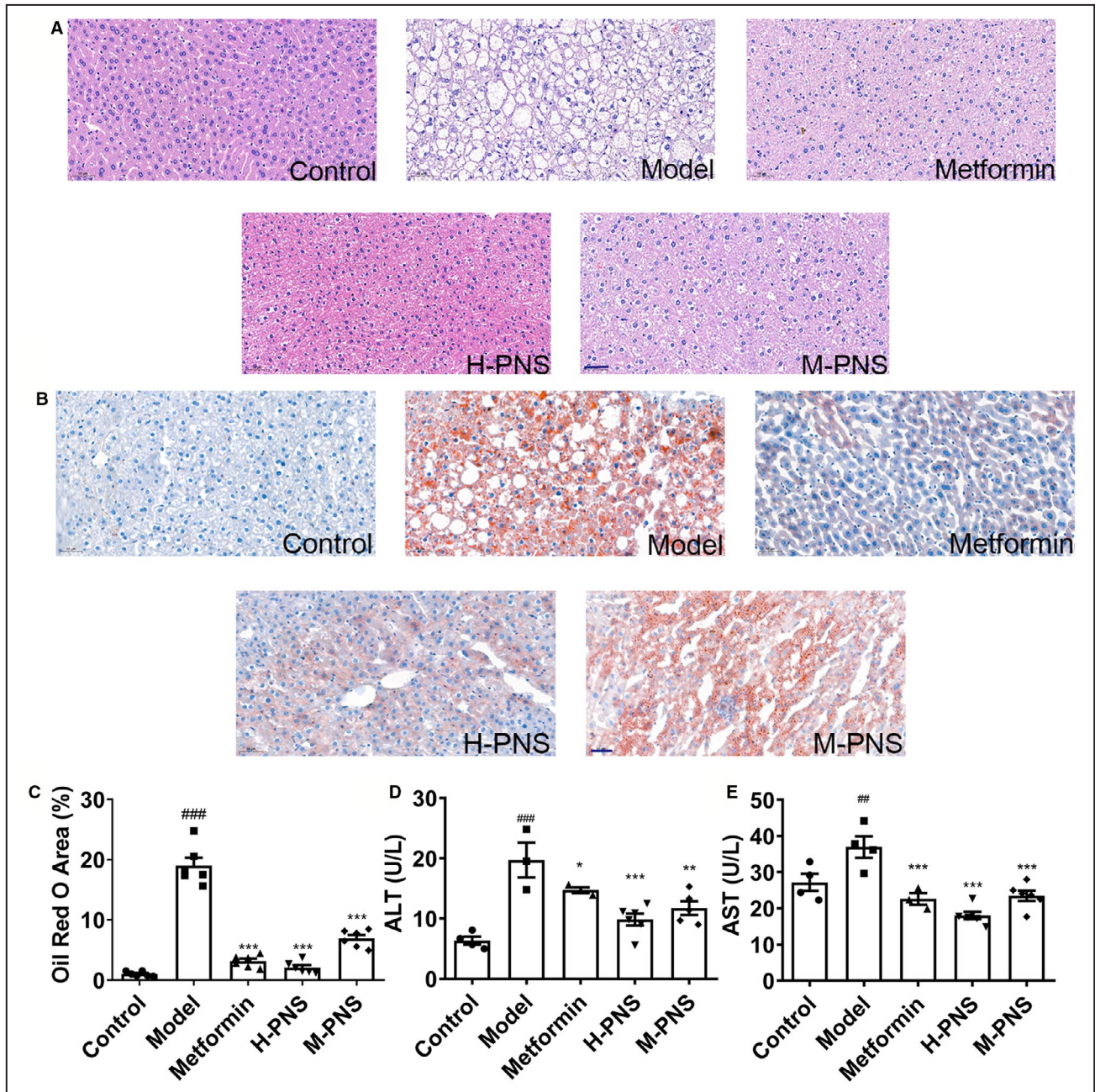


**Figure 4. PNS reduced lipid accumulation in the liver and promoted liver function.**

Representative images of (A) HE staining; (B) Oil red O staining, and (C) quantitative analysis of Oil red O stainings in 5 groups. Scale bar, 50  $\mu\text{m}$ . Data are expressed as the mean  $\pm$  SEM ( $n=6$ ). \*\*\* $P < 0.001$  vs model group; ### $P < 0.001$  vs the control. Serum (D) ALT and (E) AST levels in different groups. Data are expressed as the mean  $\pm$  SEM ( $n=3-6$ ). \* $P < 0.05$  or \*\* $P < 0.01$  or \*\*\* $P < 0.001$  vs model group; ## $P < 0.01$  or ### $P < 0.001$  vs the control. ALT indicates alanine aminotransferase; AST, aspartate aminotransferase; HE, hematoxylin and eosin; H-PNS, db/db+PNS 200 mg/kg per day group; M-PNS, db/db+PNS 100 mg/kg per day group; and PNS, *Panax notoginseng* saponin.



in the model group compared with that of the control group (Figure 5B and 5C,  $P<0.05$ ), which demonstrated the occurrence of dilated cardiomyopathy by week 36. In the PNS-treated groups, these parameters significantly decreased compared with that of the model group ( $P<0.05$ ). LVAW, LVPW, and LV volume in diastolic end in diabetic mice were also improved by PNS treatment (Figure 5D through 5F,  $P<0.05$ ). EF and FS were significantly lower in diabetic mice than in control mice (Figure 5G through 5H,  $P<0.05$ ), indicating decreased diastolic dysfunction in diabetic mice. However, PNS administration significantly improved these parameters ( $P<0.05$ ), indicating that PNS can alleviate heart failure in diabetic mice. Although metformin administration improved EF and FS ( $P<0.05$ ), it did not significantly improve LVID in systolic end in the model group ( $P>0.05$ ).

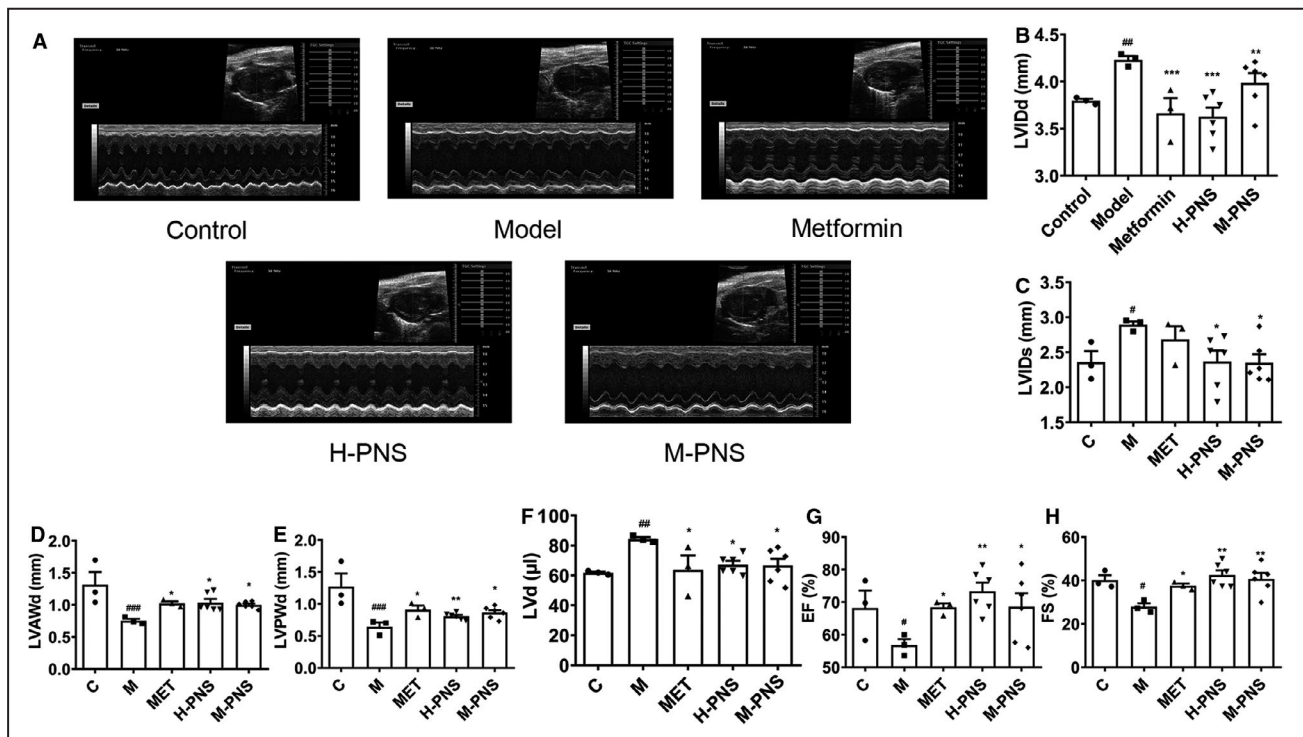
### PNS Attenuated Cardiac Fibrosis and Hypertrophy in Diabetic Mice

Figure 6A through 6C show representative images of HE, Masson, and TUNEL staining. Increased cross-sectional areas and interstitial fibrosis of atrial cardiomyocytes were observed in diabetic mice (Figure 6D and 6E,  $P<0.001$ ), which were attenuated by PNS and metformin treatments ( $P<0.001$ ). Increased inflammatory cell infiltration and mineralization were observed in the diabetic heart, but PNS and metformin administration improved cardiac morphology. TUNEL staining showed significantly increased apoptosis in the model group (Figure 6F,  $P<0.001$ ), whereas PNS and metformin treatment decreased the apoptotic rate in diabetic hearts. Serum CK, CK-MB, and LDH levels at the week 36 were higher in the model group than in the control or other treatment groups (Figure 6G through 6I,  $P<0.05$ ). PNS treatment significantly lowered serum CK and LDH levels in diabetic mice ( $P<0.01$ ). Although H-PNS significantly improved CK-MB levels in mice with diabetes ( $P<0.01$ ), the difference was not statistically significant between the M-PNS and model groups ( $P>0.05$ ). Metformin improved only CK levels in diabetic mice ( $P<0.001$ ); CK-MB and LDH levels were not decreased by metformin treatment ( $P>0.05$ ). These data demonstrated that PNS administration alleviated cardiac dysfunction in diabetic mice by reducing hypertrophy, fibrosis, and apoptosis.

### PNS Promoted Lipid and Glucose Metabolism in Diabetic Heart

To explore the effects of PNS on lipid droplet formation, Oil Red O staining was used to quantify lipid accumulation in cardiomyocytes (Figure 7A). A larger number of lipid droplets were observed in the hearts of db/db mice, and PNS and metformin administration improved lipid

accumulation in diabetic hearts (Figure 7B,  $P<0.001$ ). To confirm this result, H9c2 cells were cultured with PA to induce lipotoxicity. The 300  $\mu\text{mol/L}$  PA-treated cells were used as the model group, and 100  $\mu\text{g/mL}$  PNS (H-PNS) and 50  $\mu\text{g/mL}$  PNS (M-PNS) were used for further experiments (Figure 7C through 7E,  $P<0.001$ ). Berberine (5  $\mu\text{mol/L}$ ) was used as a positive control because of its great lipid-lowering effects. BODIPY staining in H9c2 cells showed few small lipid droplets, whereas incubation with PA increased the number of lipid droplets ( $P<0.001$ ). However, the addition of PNS and berberine significantly decreased the number of lipid droplets compared with that of the model group, as evidenced by decreased green fluorescence in PNS- and berberine-treated H9c2 cells (Figure 7F and 7G,  $P<0.001$ ). Overall, these data indicate that PNS administration reduced the accumulation of cytosolic lipid droplets. To further elucidate the lipid-lowering mechanisms of PNS, H-PNS was used for quantitative reverse-transcription polymerase chain reaction and western blotting. Expression of genes related to lipid metabolism, such as peroxisome proliferator activated receptor  $\alpha$  (PPAR $\alpha$ ), peroxisome proliferator activated receptor  $\gamma$  coactivator 1 $\alpha$  (PGC-1 $\alpha$ ), acetyl-CoA acyltransferase 2, acyl-CoA dehydrogenase, malonyl-CoA decarboxylase, CD36, diacylglycerol acyltransferase 1, and PNPLA (patatin-like phospholipase domain-containing protein 4), significantly decreased in the diabetic heart (Figure 8A,  $P<0.01$ ). Expression of genes involved in glucose metabolism, such as glucose transporter 4, pyruvate dehydrogenase kinase 4, pyruvate dehydrogenase  $\alpha$ , and hexokinase 2, also decreased in the model group (Figure 8B,  $P<0.01$ ). H-PNS treatment significantly increased the expression of the genes except PNPLA and hexokinase 2 ( $P<0.05$ ). This suggests that PNS can improve glucose and lipid metabolism in diabetic hearts. However, metformin administration only partially improved their expression. Accordingly, in H9c2 cells, the protein levels of phosphorylated acetyl CoA carboxylase, acetyl CoA carboxylase, PGC-1 $\alpha$ , carnitine palmitoyltransferase 1a (Cpt1a), Cpt1b, Cpt2, CD36, PPAR $\alpha$ , glucose transporter 4, pyruvate dehydrogenase kinase 4, and FABP4 (fatty acid binding protein 4) were significantly decreased in the model group compared with that of the control (Figure 8C through 8F,  $P<0.01$ ). PNS treatment significantly improved their levels ( $P<0.05$ ), which reduced lipid accumulation in cardiomyocytes and provided sufficient energy for normal cardiac function. Berberine also increased the levels of proteins involved in lipid and glucose metabolism in PA-treated H9c2 cells ( $P<0.05$ ). These data indicated that PNS reduced lipid accumulation in the diabetic heart by promoting lipid metabolism, and glucose metabolism was also accelerated to alleviate insulin resistance.



**Figure 5. PNS ameliorated cardiac dysfunction in diabetic mice.**

**A**, Representative images of echocardiography from mice after 12 weeks of treatment. Statistical analyses of **(B)** LVIDd; **(C)** LVIDs; **(D)** LVAWd; **(E)** LVPWd; **(F)** LVd; **(G)** EF%, and **(H)** FS% in indicated groups. Data are expressed as the mean±SEM (n=3–6). \* $P<0.05$  or \*\* $P<0.01$  or \*\*\* $P<0.001$  vs model group; # $P<0.05$  or ## $P<0.01$  or ### $P<0.001$  vs the control. C indicates control; EF, left ventricular ejection fraction; FS, fractional shortening; H-PNS, db/db+PNS 200 mg/kg per day group; LVAWd, left ventricular anterior wall thickness in diastolic end; LVd, left ventricular volume in diastolic end; LVIDd, left ventricular internal diameter in diastolic end; LVIDs, left ventricular internal diameter in systolic end; LVPWd, left ventricular posterior wall thickness in diastolic end; M, model; MET, metformin; M-PNS, db/db+PNS 100 mg/kg per day group; and PNS, *Panax notoginseng* saponin.

## PNS Reduced ROS Accumulation in Mitochondria

Cells store free acids as triacylglycerols in lipid droplets, whereas lipid overload induces ROS generation in the mitochondria.<sup>22</sup> Serum catalase, SOD, GSH peroxidase, and malondialdehyde levels were quantified, and diabetic mice showed attenuated antioxidative function; however, their levels were increased by PNS treatment (Figure 9A through 9D,  $P<0.001$ ), whereas metformin treatment did not significantly improve the antioxidative function of diabetic mice ( $P>0.05$ ). Consistently, H9c2 cells exposed to PA showed significantly increased mitochondrial superoxide levels, as evidenced by increased fluorescence intensity in PA-treated H9c2 cells. By contrast, pretreatment with berberine or PNS reduced mitochondrial superoxide levels (Figure 9E and 9F,  $P<0.05$ ). In addition, ratio of reduced to oxidized glutathione was detected and PNS significantly reversed the decreased levels in model group, which indicated improved antioxidant function in PNS-treated H9c2 cells (Figure 9G,  $P<0.05$ ). Concomitantly, the gene expression of SOD, glutathione S-transferase, NAD(P)H:quinoneoxidoreductase 1, glutamate cysteine ligase

modifier subunit, KEAP1 (Kelch-like ECH-associated protein 1), nuclear respiratory factor 1 (NRF1), and NRF2 was significantly reduced in the model group (Figure 9H,  $P<0.01$ ), compared with that of the controls. However, the expression of SOD, glutathione S-transferase, NAD(P)H:quinoneoxidoreductase 1, glutamate cysteine ligase modifier subunit, NRF2, and NRF1 significantly increased in the H-PNS group ( $P<0.01$ ), suggesting that PNS improved the antioxidative function of cardiomyocytes, which was suppressed by PA. By contrast, metformin administration improved only glutathione S-transferase, NAD(P)H:quinoneoxidoreductase 1, glutamate cysteine ligase modifier subunit, and NRF2 levels ( $P<0.05$ ). Generally, PNS exerted excellent effects in reducing ROS accumulation and increasing antioxidant function.

## PNS Improved Mitochondrial Function, Morphology, and Membrane Potential in Diabetic Cardiomyopathy

Mitochondria are major organelles that participate in ROS generation, and mitochondrial damage has been

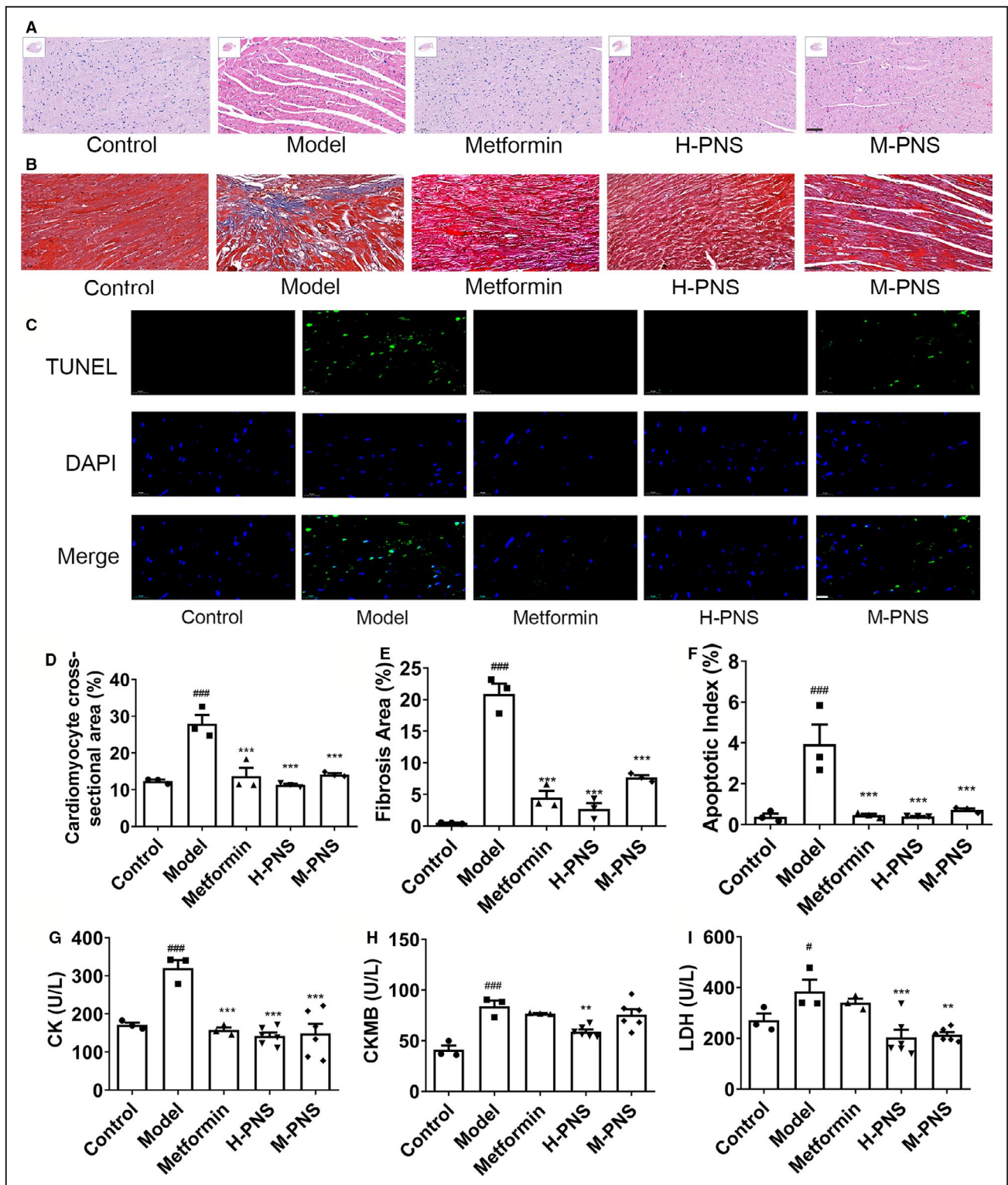


**Figure 6. PNS reduced myocardial hypertrophy, fibrosis, and apoptosis in diabetic mice.**

Cardiomyocyte cross-sectional area and fibrotic ratio were evaluated using (A) HE staining and (B) Masson staining in indicated groups. The section from which images were photographed were labeled in upper left area of each figure. Scale bar, 50  $\mu$ m. C, TUNEL staining images showing myocardial apoptosis in different groups. Scale bar, 50  $\mu$ m. Statistical analyses of cardiomyocyte (D) cross-sectional areas; (E) fibrotic ratios, and (F) apoptotic index in 5 groups. Data are expressed as the mean $\pm$ SEM (n=3). <sup>###</sup> $P$ <0.001 vs the model group; <sup>\*\*\*</sup> $P$ <0.001 vs the control. (G) CK; (H) CK-MB, and (I) LDH levels in sera of different groups. Data are expressed as the mean $\pm$ SEM (n=3–6). \* $P$ <0.05 or \*\* $P$ <0.01 or \*\*\* $P$ <0.001 vs model group; # $P$ <0.05 or <sup>###</sup> $P$ <0.001 vs the control. CK indicates creatine kinase; CK-MB, creatine kinase-MB; HE, hematoxylin and eosin; H-PNS, db/db+PNS 200 mg/kg per day group; LDH, lactate dehydrogenase; M-PNS, db/db+PNS 100 mg/kg per day group; PNS, *Panax notoginseng* saponin; and TUNEL, TdT-mediated dUTP nick-end labeling.

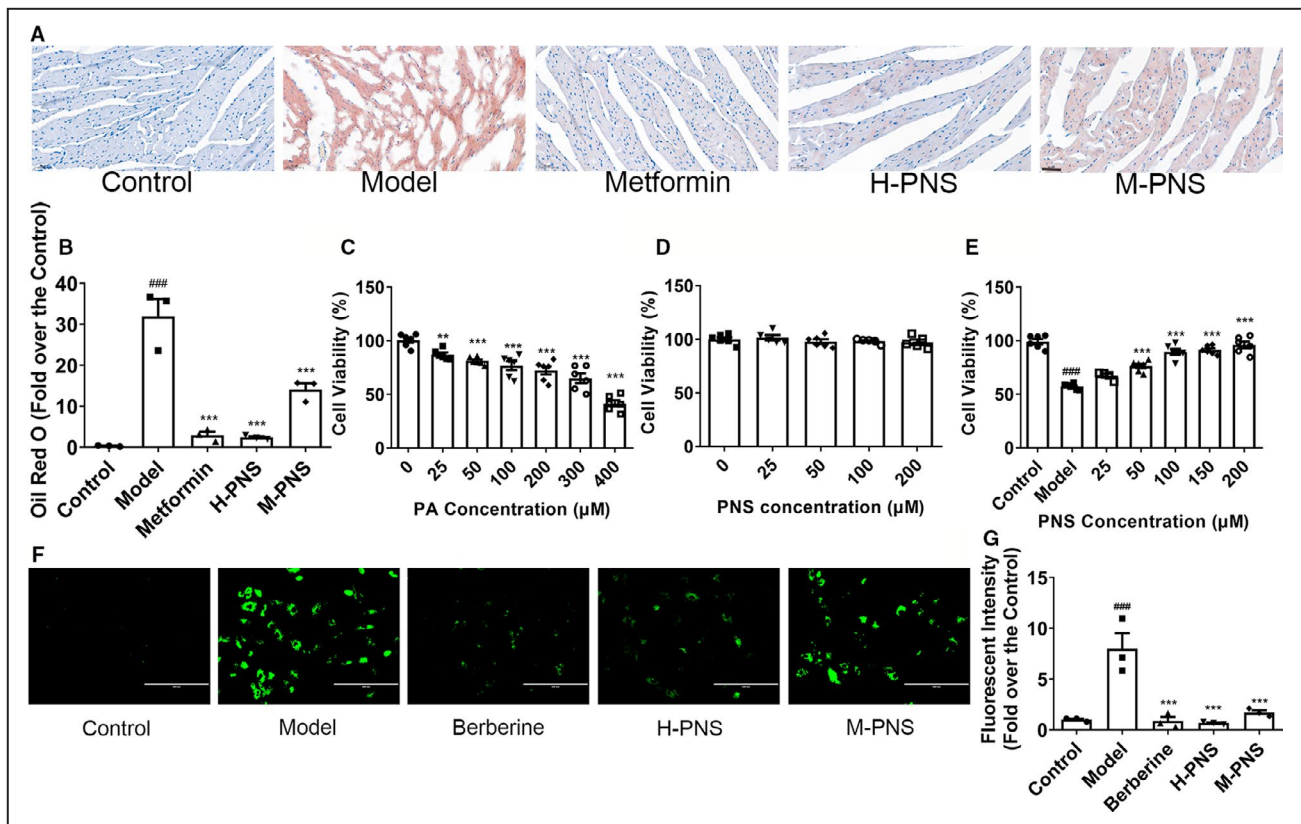


**Figure 7. PNS ameliorated lipotoxicity in diabetic heart.**

**A**, Representative images of Oil red O staining and **(B)** quantitative analysis of Oil red O staining in 5 groups. Scale bar, 50  $\mu\text{m}$ . Data are expressed as the mean $\pm$ SEM ( $n=3$ ). \*\*\* $P<0.001$  vs model group; ### $P<0.001$  vs the control. Cell viability measured using MTT assay showing **(C)** PA toxicity, **(D)** PNS toxicity, and **(E)** PNS availability. Data are expressed as the mean $\pm$ SEM ( $n=6$ ). \*\* $P<0.01$  or \*\*\* $P<0.001$  vs model group; ### $P<0.001$  vs the control. **F**, Representative images of BODIPY staining **(G)** and quantitative analysis of green fluorescence in H9c2 cells. Scale bar, 100  $\mu\text{m}$ . Data are expressed as the mean $\pm$ SEM ( $n=3$ ). \*\*\* $P<0.001$  vs model group; ### $P<0.001$  vs the control. H-PNS indicates db/db+PNS 200 mg/kg per day group; M-PNS, db/db+PNS 100 mg/kg per day group; MTT, 5-diphenyltetrazolium bromide; PA, palmitate acid; and PNS, *Panax notoginseng* saponin.

related to the occurrence of several cardiovascular diseases.<sup>23</sup> Transmission electron microscopy images showed an obvious alteration in the morphological appearance of mitochondria in the hearts of diabetic mice, indicating mitochondrial damage (Figure 10A). To confirm whether PNS has protective effects on mitochondria in diabetic cardiomyopathy, the appearance of mitochondria, such as mitochondrial size, was analyzed (Figure 10B). The results demonstrated that PNS and metformin increased mitochondrial size in diabetic hearts ( $P<0.01$ ), indicating alleviated mitochondrial fission. To confirm the protective effect of PNS on mitochondria, H9c2 cells were stained with fluorescent dye after treated with PA, mitochondrial content and membrane potential were evaluated. In the PA-treated group, mitochondrial content decreased, as shown by attenuated red fluorescence, whereas PNS and berberine treatments increased mitochondrial content in PA-treated cells (Figure 10C and 10D,  $P<0.05$ ). The fluorescence of JC-1 represented  $\Delta\Psi_m$  of mitochondria, red represented aggregates and high potential, and

green represented monomers and low potential. The fluorescence intensities indicated that PA treatment significantly reduced  $\Delta\Psi_m$ , whereas berberine and PNS pretreatments successfully attenuated the  $\Delta\Psi_m$  reduction induced by PA (Figure 10E and 10F,  $P<0.05$ ). As H-PNS showed greater effects than M-PNS in protecting against mitochondrial dysfunction, H-PNS was used for further evaluation of mitochondrial function. PA pretreatment significantly suppressed the mitochondrial respiratory capacity including basal respiration, maximal respiration, and spare respiration, of whom maximal respiration and spare respiration were significantly improved by pre-treating with PNS (Figure 11A and 11B,  $P<0.05$ ). Correspondingly, expression of genes involved in mitochondrial respiration and dynamics significantly decreased in the model group, succinate dehydrogenase enzyme subunit A (*Sdha*), *ATP5j*, *ATP5h*, *dynamin-related protein 1 (Drp1)*, *Sirt1*, *mitofusin 2 (Mfn2)*, *Mfn1*, and *Opa1*, while metformin and PNS pretreatment significantly improved the expression of these genes except *Sirt1* (Figure 11C;  $P<0.05$ ).

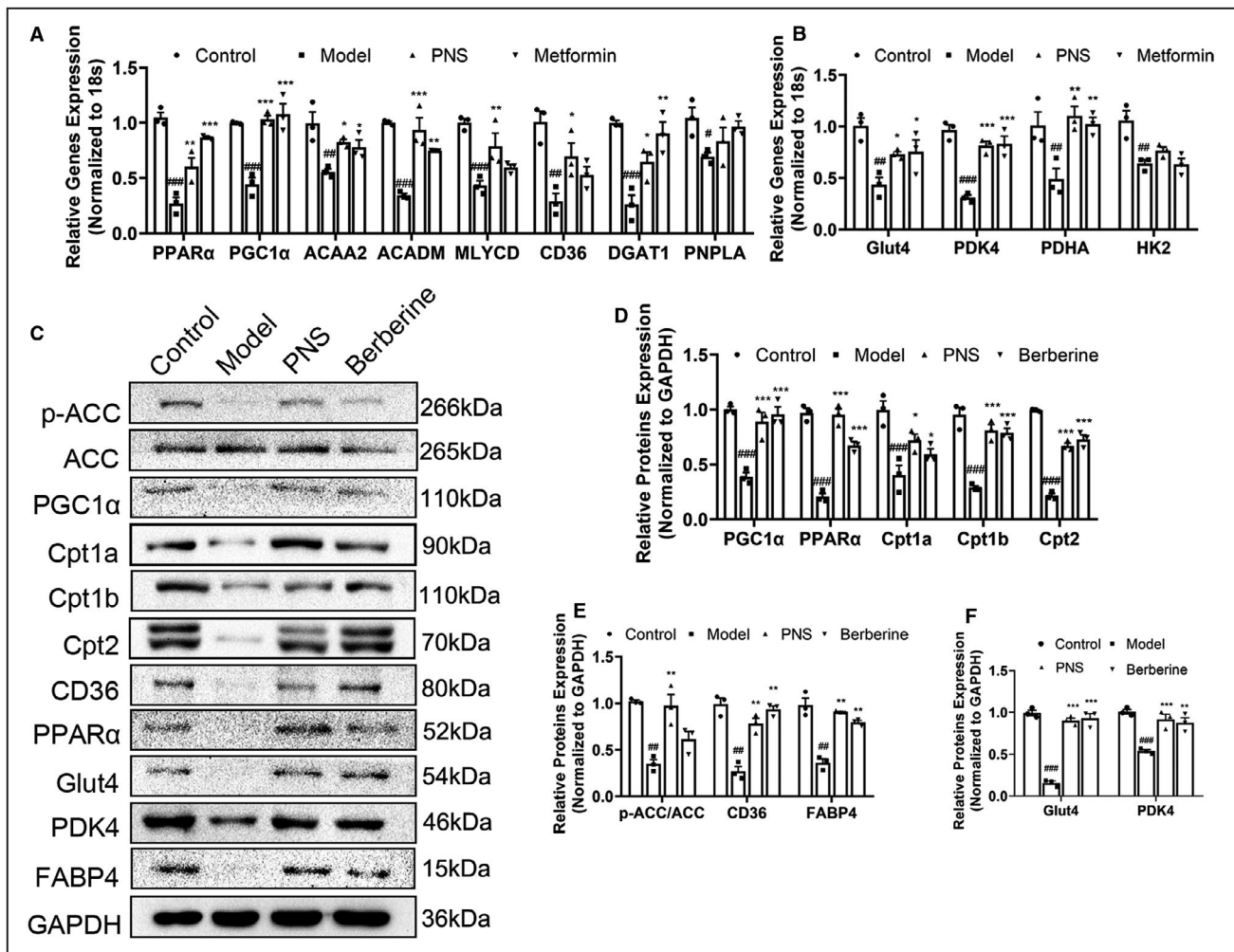


**Figure 8. PNS regulated lipid and glucose metabolism in diabetic heart.**

Transcription levels of genes involved in (A) lipid metabolism and (B) glucose metabolism in indicated 4 groups. (C) Representative blot images of proteins related to lipid metabolism and quantitative analysis of protein levels including (D) fatty acid  $\beta$ -oxidation, (E) synthesis and transportation of fatty acids, and (F) glucose metabolism. Data are expressed as the mean  $\pm$  SEM (n=3). \* $P$ <0.05 or \*\* $P$ <0.01 or \*\*\* $P$ <0.001 vs model group; # $P$ <0.05 or ## $P$ <0.01 or ### $P$ <0.001 vs the control. ACAA2 indicates acetyl-CoA acyltransferase 2; ACADM, acyl-CoA dehydrogenase; Cpt1a, carnitine palmitoyltransferase 1a; DGAT1, diacylglycerol acyltransferase 1; Glut4, glucose transporter 4; MLYCD, malonyl-CoA decarboxylase; p-ACC, phosphorylated acetyl CoA carboxylase; PDHA, pyruvate dehydrogenase  $\alpha$ ; PDK4, pyruvate dehydrogenase kinase 4; PGC-1 $\alpha$ , peroxisome proliferator activated receptor  $\gamma$  coactivator 1 $\alpha$ ; PNS, *Panax notoginseng* saponin; and PPAR $\alpha$ , peroxisome proliferator activated receptor  $\alpha$ .

Consistently, the protein levels of Mfn2 and TFAM (transcription factor A mitochondrial) were significantly reduced in the model group (Figure 11D and 11E, 11G,  $P$ <0.001), in comparison to that of the control group. PNS and berberine treatment increased their levels, which indicated increased mitochondrial biogenesis and fusion in PNS-treated diabetic mice ( $P$ <0.01). The level of mitochondrial division protein was higher in the model group than in the controls, while PNS and berberine treatments decreased its level, which demonstrated decreased mitochondrial fission in berberine and PNS-treated groups (Figure 11D and 11F,  $P$ <0.01). These data demonstrate that PNS improves mitochondrial function by reducing mitochondrial fission,

promoting mitochondrial fusion and genesis, and maintaining mitochondrial membrane potential.

## DISCUSSION

Obesity is defined as excessive body fat accumulation, which has been shown to be associated with type 2 diabetes.<sup>24</sup> Excess adipose tissue or ectopic fat accumulation in the liver causes insulin resistance.<sup>25</sup> Adipose and liver dysfunction are related to disturbed lipid metabolism, which is the cause of numerous cardiovascular diseases.<sup>26</sup> Diabetic cardiomyopathy is characterized by increased lipid use and oxidation, which leads to cardiac lipotoxicity.<sup>4</sup> Excessive fatty

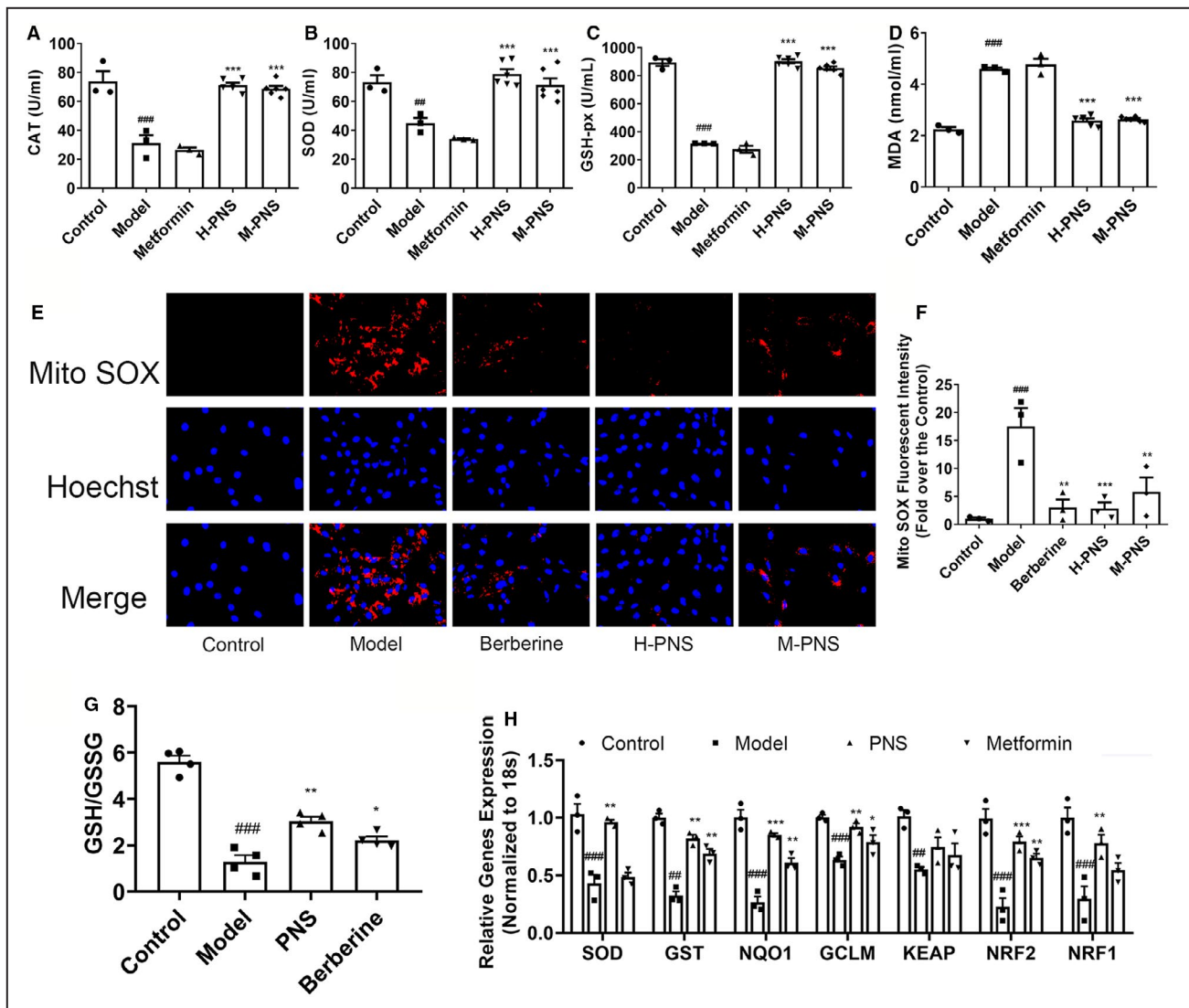


**Figure 9. PNS treatment reduced oxidative stress in diabetic heart.**

**A**, CAT; **(B)** SOD; **(C)** GSH-px, and **(D)** MDA levels in sera of mice from 5 groups. Data are expressed as the mean±SEM (n=3–6). \*\*\* $P$ <0.001 vs model group; ## $P$ <0.01 or ### $P$ <0.001 vs the control. **E**, Representative images of mitochondrial reactive oxygen species (ROS) in H9c2 cells visualized using MitoSOX and **(F)** quantitative analysis of mitochondrial ROS in 5 groups. Scale bar, 100  $\mu$ m. Data are expressed as the mean±SEM (n=3). \* $P$ <0.05 vs model group; ## $P$ <0.01 vs the control. **G**, Ratio of GSH ad GSSG in PNS and PA-treated H9c2 cells. Data are expressed as the mean±SEM (n=4). \* $P$ <0.05 or \*\* $P$ <0.01 vs model group; ### $P$ <0.001 vs the control. **H**, Transcription levels of genes related to oxidative stress response and ROS metabolism in indicated groups. Data are expressed as the mean±SEM (n=3). \* $P$ <0.05 or \*\* $P$ <0.01 or \*\*\* $P$ <0.001 vs model group; ## $P$ <0.01 or ### $P$ <0.001 vs the control. CAT indicates catalase; GCLM, glutamate cysteine ligase modifier subunit; GSH-px, glutathione peroxidase; GSSG, oxidized glutathione; GST, glutathione S-transferase; H-PNS indicates db/db+PNS 200 mg/kg per day group; KEAP1, Kelch-1-like ECH-associated protein 1; MDA, malondialdehyde; M-PNS, db/db+PNS 100 mg/kg per day group; NQO1, NAD(P)H:quinoneoxidoreductase 1; NRF1, nuclear respiratory factor 1; PA, palmitate acid; PNS, *Panax notoginseng* saponin; and SOD, superoxide dismutase.

acid oxidation in the mitochondria causes accumulation of ROS that cannot be scavenged, which further leads to mitochondrial dysfunction.<sup>27</sup> Damaged mitochondria reduce the capacity for oxidation of substrates, which causes inadequate energy supply to cardiomyocytes, finally leading to heart failure.<sup>28</sup> Therefore, diverse approaches that promote free acid oxidation, ROS scavenging, or mitogenesis can alleviate lipid-induced cardiac dysfunction.<sup>4</sup> In this study,

diabetic mice were treated with PNS, which ameliorated diabetic cardiomyopathy by modulating lipid metabolism, thereby reducing oxidative stress and promoting mitochondrial function, which alleviated heart failure.

In this study, PNS supplementation in diabetic mice showed significant inhibitory effect on weight gain and lipid accumulation in the liver and adipose tissue. Additionally, PNS administration significantly lowered

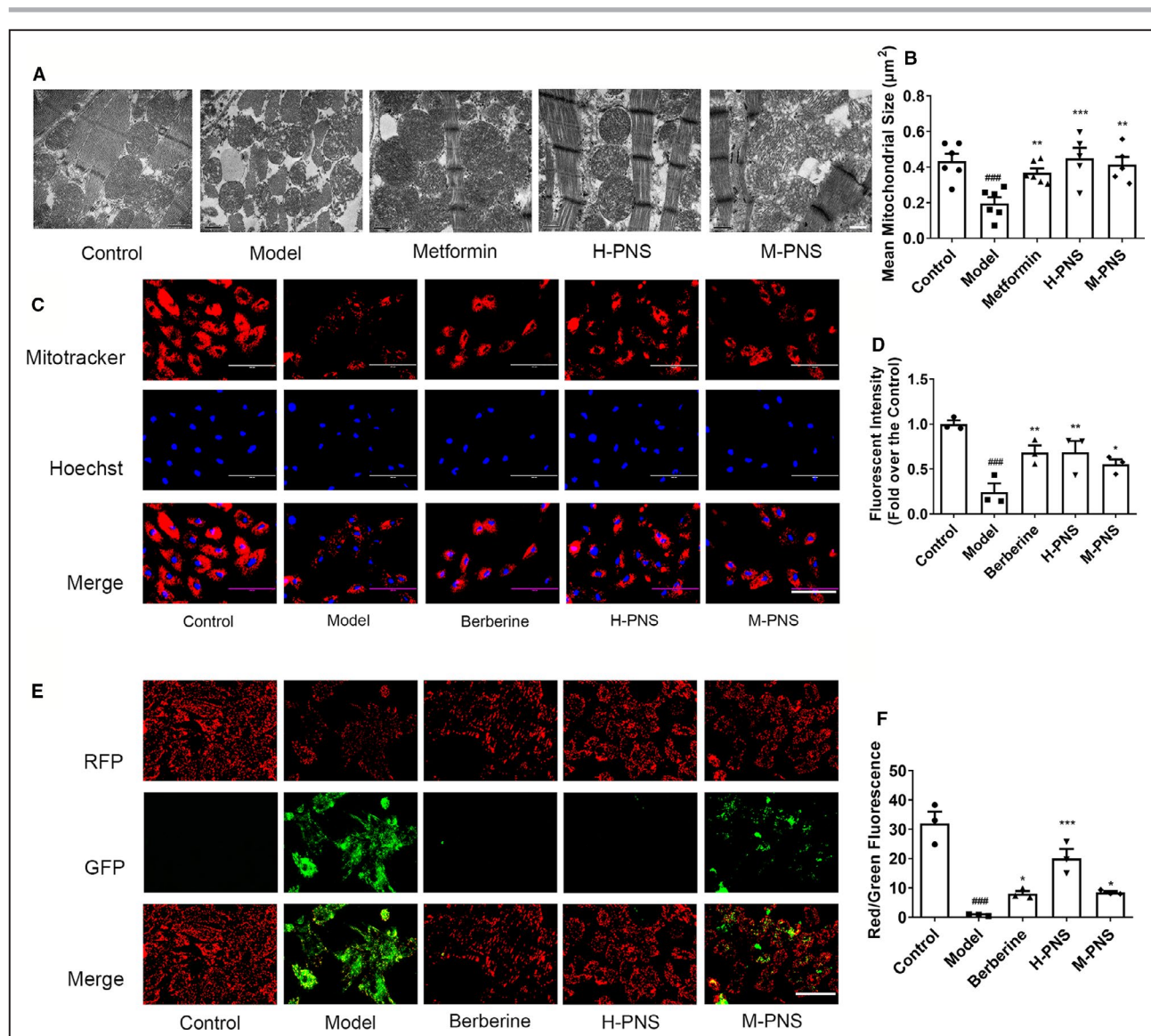


**Figure 10. PNS treatment improved myocardial mitochondrial morphology and cell viability.**

**A**, Representative transmission electron microscopy images. Scale bar, 0.5 µm. **B**, Quantitative analysis of mitochondrial size. Data are expressed as the mean±SEM (n=6). \*\* $P < 0.01$  or \*\*\* $P < 0.001$  vs. model group; ### $P < 0.001$  vs. the control. **(C)** Representative images of mitochondria stained using MitoTracker Red. Scale bar, 100 µm. **(D)** Quantitative analysis of mitochondrial number calculated using fluorescence intensity. Data are expressed as the mean±SEM (n=3). \* $P < 0.05$  or \*\* $P < 0.01$  vs. model group; ### $P < 0.001$  vs. the control. **(E)** Representative images of mitochondrial membrane potential stained using JC-1 in H9c2 cardiomyocytes. Scale bar, 100 µm. **(F)** Quantitative analysis of mitochondrial membrane potential shown by ratio of red and green fluorescence. Data are expressed as the mean±SEM (n=3). \* $P < 0.05$  or \*\*\* $P < 0.001$  vs. model group; ### $P < 0.001$  vs. the control. GFP indicates green fluorescent protein; H-PNS db/db+PNS 200 mg/kg per day group; M-PNS, db/db+PNS 100 mg/kg per day group; PNS, *Panax notoginseng* saponin; and RFP, red fluorescent protein.

serum insulin and lipid levels and, therefore, improved adipose and liver function. There was a strong positive correlation between body fat and serum total cholesterol and TG levels. Adipocyte hypertrophy and adipose tissue dysfunction in diabetic mice reduce TG storage and lead to hyperlipidemia but reduced high-density lipoprotein levels in the serum.<sup>29</sup> Increased release of FFA from adipose tissues results in elevated hepatic

uptake, and increased serum glucose and insulin levels result in intracellular fatty acids that are not oxidized but esterified to TG and stored within lipid droplets. Furthermore, intermediates of fatty acid metabolism impair insulin signaling and promote insulin resistance,<sup>30</sup> Adipose tissue dysfunction is accompanied by adipocyte hypertrophy, reduced TG synthesis, resistance

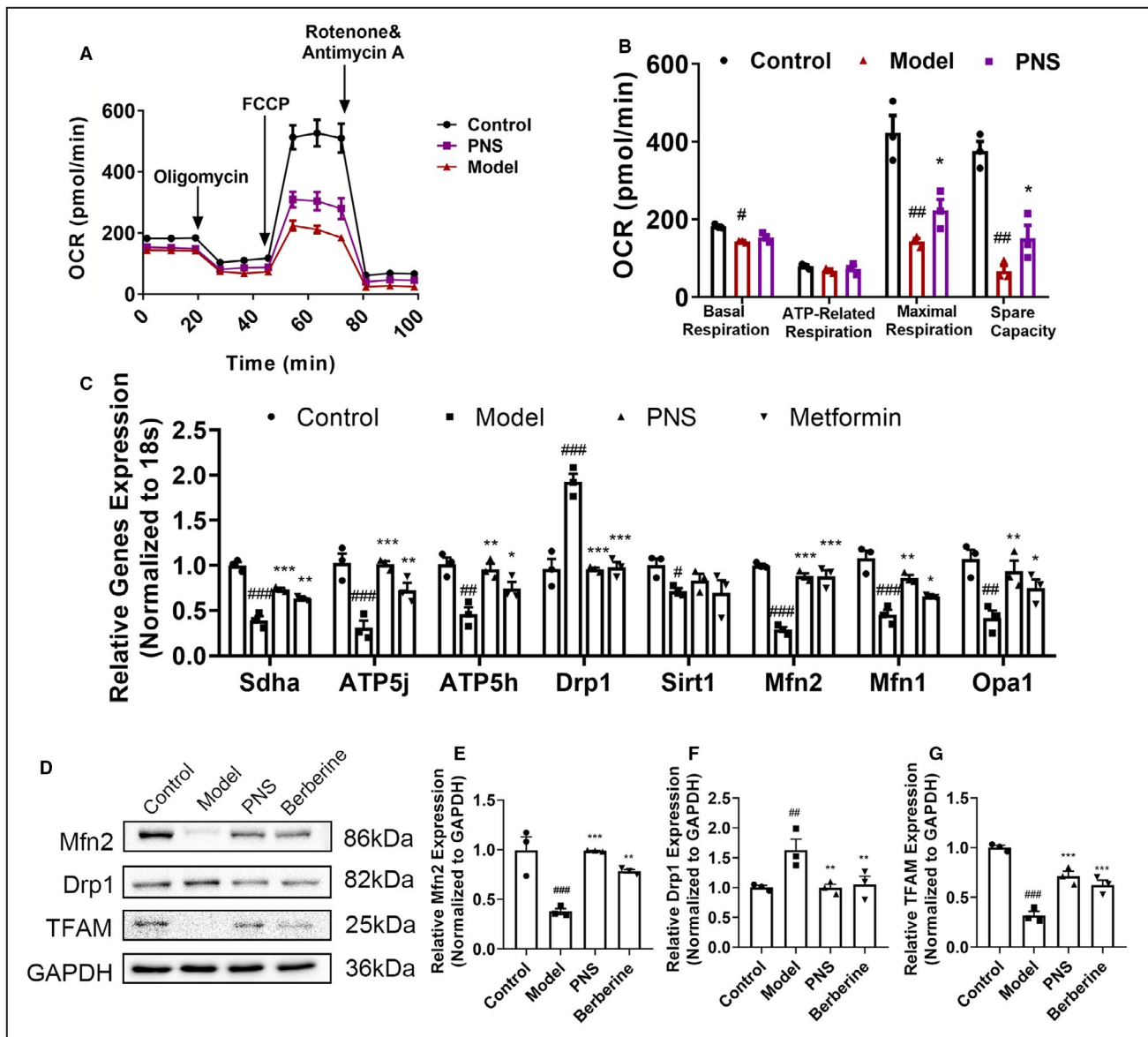


**Figure 11. PNS treatment improved myocardial mitochondrial respiration and dynamics.**

**A**, OCR and **(B)** quantitative statistical analysis of OCR. Data are expressed as the mean $\pm$ SEM (n=3). \* $P$ <0.05 vs. model group; # $P$ <0.05 or ## $P$ <0.01 vs the control. **C**, Transcription levels of genes related to mitochondrial respiration and dynamics in 4 indicated groups. Data are expressed as the mean $\pm$ SEM (n=3). \* $P$ <0.05 or \*\* $P$ <0.01 or \*\*\* $P$ <0.001 vs model group; # $P$ <0.05 or ## $P$ <0.01 or ### $P$ <0.001 vs the control. **D**, Levels of proteins related to mitochondrial biogenesis, division, and fusion estimated using western blotting. **(E)** Mfn2; **(F)** Drp1 and **(G)** TFAM protein levels in the 4 study groups. Data are expressed as the mean $\pm$ SEM (n=3). \*\* $P$ <0.01 or \*\*\* $P$ <0.001 vs model group; ## $P$ <0.01 or ### $P$ <0.001 vs the control. Drp1 indicates dynamin-related protein 1; FCCP, carbonyl cyanide p-trifluoromethoxyphenylhydrazone; Mfn2, mitofusin 2; OCR, oxygen consumption rate; Opa1, optic atrophy type 1; PNS, high-dose *Panax notoginseng* saponin; Sdha, succinate dehydrogenase enzyme subunit A; and TFAM, transcription factor A mitochondrial.

to the inhibitory effect of insulin on lipolysis, fat tissue fibrosis, immune cell infiltration, and inflammatory cytokine secretion.<sup>31</sup> High levels of tumor necrosis factor- $\alpha$  and IL-6 suppress the production of adiponectin,<sup>32</sup> which results in hepatic insulin resistance and the accumulation of liver fat.<sup>33</sup> Obesity is also accompanied by higher circulating levels of leptin,<sup>34</sup> which regulates energy intake and expenditure, metabolism, and reproductive function and prevents lipid accumulation in

the liver. Elevated aspartate aminotransferase and alanine aminotransferase levels were observed, indicating hepatic dysfunction.

Metabolic disorders associated with diabetes, such as hyperglycemia, elevated levels of circulating fatty acids, hyperinsulinemia, and increased levels of inflammatory cytokines, alter multiple molecular pathways within the cardiomyocytes, which impair cardiac contractility and promote myocyte dysfunction and



injury.<sup>35</sup> A remarkable feature of diabetic cardiomyopathy is cardiac hypertrophy, which is accompanied by weakened systolic and diastolic functions.<sup>36,37</sup> Diastolic dysfunction is an early functional remodeling in the diabetic myocardium. Systolic dysfunction may also develop but occurs mostly at a later stage of diabetes. In this study, db/db mice showed weakened myocardial contractility, as evidenced by significantly decreased LVAWd and LVPWd, and increased LVIDd and LV, which indicated diastolic dysfunction. Increased LVIDs and decreased EF and FS were also observed, which demonstrated systolic dysfunction and heart failure in the later stage of diabetic cardiomyopathy. Moreover, hypertrophy, fibrosis, and apoptosis were observed in diabetic cardiomyocytes, which further impaired cardiac function. Serum LDH, CK, and CK-MB levels have been clinically used to assess heart injury,<sup>38</sup> and elevated serum LDH, CK, and CK-MB levels were observed in diabetic mice, which indicated serious cardiac injury in diabetic mice. However, upon treatment with PNS, cardiac dysfunction was alleviated, hypertrophy, fibrosis, and apoptosis in diabetic hearts were improved, and elevated LDH, CK, and CK-MB levels were also decreased. These data indicate that PNS can protect against cardiomyopathy by improving cardiac function.

Diabetic cardiomyopathy is characterized by increased fatty acid use, which results in increased ROS production.<sup>39</sup> Although the oxidation of fatty acids normally yields significantly more energy per carbon atom than that of glucose oxidation, oxidative phosphorylation capacity is impaired in the hearts of insulin-resistant db/db mice.<sup>40</sup> If the delivery of fatty acids to the mitochondria exceeds their capacity for oxidative phosphorylation,<sup>41</sup> ceramide and diacylglycerol accumulation might lead to the development of lipotoxic cardiac dysfunction.<sup>42</sup> In this study, more numbers of lipid droplets were found in diabetic hearts and PA-treated H9c2 cells than in the control, which indicated lipotoxicity, while PNS treatment significantly reduced lipid accumulation in cardiomyocytes. Excessive lipid accumulation in cardiomyocytes was found to be due to reduced expression of adipose triglyceride lipase (ATGL) in diabetic hearts.<sup>43</sup> Concomitantly, uptake and oxidation of FFAs are reduced in diabetic hearts, most likely mediated by decreased PPAR $\alpha$  and PGC1 $\alpha$  (peroxisome proliferator-activated receptor- $\gamma$  coactivator 1 $\alpha$ ) expression.<sup>44</sup> Therefore, in this study, decreased expression of genes related to lipid uptake, use, and oxidative phosphorylation was detected in diabetic hearts, while PNS significantly increased the levels of PNPLA, PGC1 $\alpha$ , PPAR $\alpha$ , CD36, diacylglycerol acyltransferase 1, acetyl-CoA acyltransferase 2, malonyl-CoA decarboxylase, and acyl-CoA dehydrogenase. Characterized by decreased glucose use, HK2, pyruvate dehydrogenase  $\alpha$ , pyruvate dehydrogenase

kinase 4, and glucose transporter 4 expression significantly decreased in diabetic mice, while PNS administration improved glucose uptake and oxidation by increasing their expression, which provided more substrate for ATP production. Consistently, protein levels of phosphorylated acetyl CoA carboxylase, PGC1 $\alpha$ , PPAR $\alpha$ , Cpt1a, Cpt1b, Cpt2, CD36, glucose transporter 4, pyruvate dehydrogenase kinase 4, and FABP4 were significantly reduced in the model group. However, PNS treatment improved lipid accumulation in cardiomyocytes by promoting free acid oxidation, and increasing glucose and lipid uptake and use in cardiomyocytes, which promoted energy production in mitochondria.

Anderson et al. observed impaired mitochondrial respiratory capacity and increased mitochondrial oxidative stress in the atrial tissue of patients with type 2 diabetes.<sup>45,46</sup> ROS overproduction has been shown to be the major cause of diabetic and obese pathophysiology under hyperglycemic and hyperlipidemic conditions.<sup>47</sup> In db/db mice, decreased levels of SOD, catalase, and GSH-peroxidase were observed, which indicated impaired ROS scavenging. PA-treated H9c2 cells showed increased mitochondrial ROS accumulation and decreased ratio of GSH to oxidized glutathione, and the expression of antioxidant genes KEAP1, NRF2, NRF1, SOD, glutathione S-transferase, glutamate cysteine ligase modifier subunit, and NAD(P)H:quinoneoxidoreductase 1 also decreased. However, after treatment with PNS, H9c2 cells exhibited improved antioxidative function. There were also elevated levels of SOD, GSH-peroxidase, and catalase as well as decreased malondialdehyde in PNS-treated diabetic mice. These results demonstrate that PNS can improve antioxidant function in diabetic cardiomyopathy. However, sole measurement of malondialdehyde as a readout of lipid peroxidation is a limitation of the current study, measurement of other indices of lipid peroxidation such as F2-isoprostanes is warranted in the future to confirm the current findings.

Mitochondrial dysfunction has been implicated in the pathogenesis of diabetes and its complications in all tissues affected by diabetes.<sup>48</sup> Mitochondria are the main producers of ATP, and abnormal mitochondrial function leads to decreased energy production, which cannot maintain energy supply to cardiomyocytes and ultimately causes apoptosis of cardiac myocytes and heart failure.<sup>49</sup> Diabetes has a direct effect on mitochondrial morphology.<sup>50</sup> In diabetic mice, shrinking, swollen, and vacuolized mitochondria were observed, which indicated destruction of the energy supply, while PNS treatment reduced mitochondrial damage and reconstructed energy production. To further confirm the protective role of PNS in mitochondria, H9c2 cells were cultured. The quantity and quality of mitochondria are essential for maintaining normal cardiac function,

and normal mitochondrial membrane potential is a prerequisite for maintaining mitochondrial oxidative phosphorylation and ATP production.<sup>51,52</sup> Therefore, the content and membrane potential of mitochondria in cells treated with PA or PNS were detected using MitoTracker Red and JC-1 staining, respectively. PA treatment significantly reduced mitochondrial number and membrane potential, which demonstrated damaged mitochondrial function, BS PNS protected H9c2 cells from decreased mitochondrial number and reduced mitochondrial membrane potential, as evidenced by elevated mitochondrial function. The respiratory capacity of H9c2 cells with or without PNS treatment before PA incubation was also determined by oxygen consumption rate. PNS treatment significantly reversed the damaged respiratory capacity of H9c2 cells after PA incubation, which retained the energy supply to the cardiomyocytes. Mitochondrial dynamic cycling balances fission and fusion, which are essential for maintaining various cellular functions.<sup>53</sup> A group of dynamin-related large GTPases regulates mitochondrial morphological changes, including Drp1 and Mfn. Drp1 causes the shrinking of the mitochondrial membrane during fission, whereas Mfn supports the fusion of the outer and inner mitochondrial membranes.<sup>54</sup> Hyperglycemia induces the formation of short and small mitochondria by promoting the expression of the fission protein Drp1 and suppressing the expression of the fusion protein Mfn2, supporting a pro-fission phenotype of mitochondrial morphology.<sup>55</sup> In this study, diabetic mice exhibited smaller and deformed mitochondria in their hearts; concomitantly, the expression of Mfn2 decreased, whereas that of Drp1 increased in the model group. Additionally, TFAM expression was significantly decreased in diabetic mice, indicating impaired mitogenesis. However, PNS reversed these changes, indicating that PNS may protect against mitochondrial dysfunction.

## CONCLUSIONS

PNS treatment improved cardiac function in diabetic mice by modulating lipid metabolism, as well as preventing oxidative stress and protecting mitochondrial function in cardiomyocytes. Therefore, PNS may be a promising drug for treating diabetic cardiomyopathy.

## ARTICLE INFORMATION

Received August 6, 2021; accepted December 9, 2021.

### Affiliations

Beijing Key Laboratory of Innovative Drug Discovery of Traditional Chinese Medicine (Natural Medicine) and Translational Medicine, Institute of Medicinal Plant Development, Peking Union Medical College and Chinese Academy of Medical Sciences, Beijing, China; Key Laboratory of Bioactive Substances

and Resource Utilization of Chinese Herbal Medicine, Ministry of Education, Beijing, China; Key Laboratory of Efficacy Evaluation of Chinese Medicine against Glycolipid Metabolic Disorders; NMPA Key Laboratory for Research and Evaluation of Pharmacovigilance; Zhongguancun Open Laboratory of the Research and Development of Natural Medicine and Health Products and Key Laboratory of New Drug Discovery Based on Classic Chinese Medicine Prescription, Chinese Academy of Medical Sciences, Beijing, China.

### Sources of Funding

This research was funded by National Natural Science Foundation of China (Grant No. 81773936), CAMS Innovation Fund for Medical Sciences (CIFMS) (Grant No. 2020-I2 M-2-01), Key Laboratory Project of CAMS (Grant No. 2018PT35030), Key R&D projects in Guangdong Province (Grant No. 2020B1111110002), and Major Program of the National Natural Science Foundation of China (Grant No. 81891012).

### Disclosures

None.

### Supplemental Material

Table S1

## REFERENCES

- DeFronzo RA. Banting lecture. From the triumvirate to the ominous octet: a new paradigm for the treatment of type 2 diabetes mellitus. *Diabetes*. 2009;58:773–795. doi: 10.2337/db09-9028
- Wewer Albrechtsen NJ, Pedersen J, Galsgaard KD, Winther-Sorensen M, Suppli MP, Janah L, Gromada J, Vilstrup H, Knop FK, Holst JJ. The liver-alpha-cell axis and type 2 diabetes. *Endocr Rev*. 2019;40:1353–1366. doi: 10.1210/er.2018-00251
- Malin SK, Kashyap SR, Hammel J, Miyazaki Y, DeFronzo RA, Kirwan JP. Adjusting glucose-stimulated insulin secretion for adipose insulin resistance: an index of beta-cell function in obese adults. *Diabetes Care*. 2014;37:2940–2946. doi: 10.2337/dc13-3011
- Bugger H, Abel ED. Molecular mechanisms of diabetic cardiomyopathy. *Diabetologia*. 2014;57:660–671. doi: 10.1007/s00125-014-3171-6
- Dillmann WH. Diabetic cardiomyopathy. *Circ Res*. 2019;124:1160–1162. doi: 10.1161/CIRCRESAHA.118.314665
- Wu MS, Liang JT, Lin YD, Wu ET, Tseng YZ, Chang KC. Aminoguanidine prevents the impairment of cardiac pumping mechanics in rats with streptozotocin and nicotinamide-induced type 2 diabetes. *Br J Pharmacol*. 2008;154:758–764. doi: 10.1038/bjp.2008.119
- Forcheron F, Basset A, Abdallah P, Del Carmine P, Gadot N, Beylot M. Diabetic cardiomyopathy: effects of fenofibrate and metformin in an experimental model—the Zucker diabetic rat. *Cardiovasc Diabetol*. 2009;8:16. doi: 10.1186/1475-2840-8-16
- Rosen R, Rump AF, Rosen P. The ace-inhibitor captopril improves myocardial perfusion in spontaneously diabetic (BB) rats. *Diabetologia*. 1995;38:509–517. doi: 10.1007/BF00400718
- Turan B. A comparative summary on antioxidant-like actions of timolol with other antioxidants in diabetic cardiomyopathy. *Curr Drug Deliv*. 2016;13:418–423. doi: 10.2174/1567201813666151123103354
- Shigeta T, Aoyama M, Bando YK, Monji A, Mitsui T, Takatsu M, Cheng X-W, Okumura T, Hirashiki A, Nagata K, et al. Dipeptidyl peptidase-4 modulates left ventricular dysfunction in chronic heart failure via angiogenesis-dependent and -independent actions. *Circulation*. 2012;126:1838–1851. doi: 10.1161/CIRCULATIONAHA.112.096479
- Lee MMY, McMurray JJV, Lorenzo-Almoros A, Kristensen SL, Sattar N, Jhund PS, Petrie MC. Diabetic cardiomyopathy. *Heart*. 2019;105:337–345. doi: 10.1136/heartjnl-2016-310342
- Yang X, Xiong X, Wang H, Wang J. Protective effects of panax notoginseng saponins on cardiovascular diseases: a comprehensive overview of experimental studies. *Evid Based Complement Alternat Med*. 2014;2014:1–13. doi: 10.1155/2014/204840
- Chen ZH, Li J, Liu J, Zhao Y, Zhang P, Zhang MX, Zhang L. Saponins isolated from the root of panax notoginseng showed significant anti-diabetic effects in KK-ay mice. *Am J Chin Med*. 2008;36:939–951. doi: 10.1142/S0192415X08006363
- Yang CY, Wang J, Zhao Y, Shen L, Jiang X, Xie ZG, Liang N, Zhang L, Chen ZH. Anti-diabetic effects of panax notoginseng saponins

- and its major anti-hyperglycemic components. *J Ethnopharmacol*. 2010;130:231–236. doi: 10.1016/j.jep.2010.04.039
15. Chen J, Xue R, Li L, Xiao LL, Shangguan J, Zhang W, Bai X, Liu G, Li L. Panax notoginseng saponins protect cardiac myocytes against endoplasmic reticulum stress and associated apoptosis through mediation of intracellular calcium homeostasis. *Front Pharmacol*. 2019;10:1013. doi: 10.3389/fphar.2019.01013
  16. Wang L, Chen X, Wang Y, Zhao L, Zhao X, Wang Y. MiR-30c-5p mediates the effects of panax notoginseng saponins in myocardial ischemia reperfusion injury by inhibiting oxidative stress-induced cell damage. *Biomed Pharmacother*. 2020;125:109963. doi: 10.1016/j.biopha.2020.109963
  17. Chen S, Liu J, Liu X, Fu Y, Zhang M, Lin Q, Zhu J, Mai L, Shan Z, Yu X, et al. Panax notoginseng saponins inhibit ischemia-induced apoptosis by activating PI3K/Akt pathway in cardiomyocytes. *J Ethnopharmacol*. 2011;137:263–270. doi: 10.1016/j.jep.2011.05.011
  18. Yue QX, Xie FB, Song XY, Wu WY, Jiang BH, Guan SH, Yang M, Liu X, Guo DA. Proteomic studies on protective effects of salvianolic acids, notoginsenosides and combination of salvianolic acids and notoginsenosides against cardiac ischemic-reperfusion injury. *J Ethnopharmacol*. 2012;141:659–667. doi: 10.1016/j.jep.2011.08.044
  19. Ning K, Jiang L, Hu T, Wang X, Liu A, Bao Y. ATP-sensitive potassium channels mediate the cardioprotective effect of panax notoginseng saponins against myocardial ischaemia-reperfusion injury and inflammatory reaction. *Biomed Res Int*. 2020;2020:1–12. doi: 10.1155/2020/3039184
  20. Wang D, Lv L, Xu Y, Jiang K, Chen F, Qian J, Chen M, Liu G, Xiang Y. Cardioprotection of panax notoginseng saponins against acute myocardial infarction and heart failure through inducing autophagy. *Biomed Pharmacother*. 2021;136:111287. doi: 10.1016/j.biopha.2021.111287
  21. Li Y, Zhao X, Feng X, Liu X, Deng C, Hu CH. Berberine alleviates olanzapine-induced adipogenesis via the ampkalpha-srebp pathway in 3t3-l1 cells. *Int J Mol Sci*. 2016;17. doi: 10.3390/ijms17111865
  22. Reynolds MS, Hancock CR, Ray JD, Kener KB, Draney C, Garland K, Hardman J, Bikman BT, Tessem JS. Beta-cell deletion of Nr4a1 and Nr4a3 nuclear receptors impedes mitochondrial respiration and insulin secretion. *Am J Physiol Endocrinol Metab*. 2016;311:E186–E201. doi: 10.1152/ajpendo.00022.2016
  23. Cadenas S. ROS and redox signaling in myocardial ischemia-reperfusion injury and cardioprotection. *Free Radic Biol Med*. 2018;117:76–89. doi: 10.1016/j.freeradbiomed.2018.01.024
  24. Gonzalez-Muniesa P, Martinez-Gonzalez MA, Hu FB, Despres JP, Matsuzawa Y, Loos RJF, Moreno LA, Bray GA, Martinez JA. Obesity. *Nat Rev Dis Primers*. 2017;3:17034. doi: 10.1038/nrdp.2017.34
  25. Fabbrini E, Magkos F, Mohammed BS, Pietka T, Abumrad NA, Patterson BW, Okunade A, Klein S. Intrahepatic fat, not visceral fat, is linked with metabolic complications of obesity. *Proc Natl Acad Sci USA*. 2009;106:15430–15435. doi: 10.1073/pnas.0904944106
  26. Amato MC, Giordano C, Galia M, Criscimanna A, Vitabile S, Midiri M, Galluzzo A, AlkaMeSy Study G. Visceral adiposity index: a reliable indicator of visceral fat function associated with cardiometabolic risk. *Diabetes Care*. 2010;33:920–922. doi: 10.2337/dc09-1825
  27. Ljubkovic M, Gressette M, Bulat C, Cavar M, Bakovic D, Fabijanic D, Grkovic I, Lemaire C, Marinovic J. Disturbed fatty acid oxidation, endoplasmic reticulum stress, and apoptosis in left ventricle of patients with type 2 diabetes. *Diabetes*. 2019;68:1924–1933. doi: 10.2337/db19-0423
  28. Bedi KC, Snyder NW, Brandimarto J, Aziz M, Mesaros C, Worth AJ, Wang LL, Javaheri A, Blair IA, Margulies KB, et al. Evidence for intramyocardial disruption of lipid metabolism and increased myocardial ketone utilization in advanced human heart failure. *Circulation*. 2016;133:706–716. doi: 10.1161/CIRCULATIONAHA.115.017545
  29. Milic S, Lulic D, Stimac D. Non-alcoholic fatty liver disease and obesity: biochemical, metabolic and clinical presentations. *World J Gastroenterol*. 2014;20:9330–9337. doi: 10.3748/wjg.v20.i28.9330
  30. Fabbrini E, Sullivan S, Klein S. Obesity and nonalcoholic fatty liver disease: biochemical, metabolic, and clinical implications. *Hepatology*. 2010;51:679–689. doi: 10.1002/hep.23280
  31. Lessard J, Laforest S, Pelletier M, Leboeuf M, Blackburn L, Tchernof A. Low abdominal subcutaneous preadipocyte adipogenesis is associated with visceral obesity, visceral adipocyte hypertrophy, and a dysmetabolic state. *Adipocyte*. 2014;3:197–205. doi: 10.4161/adip.29385
  32. Weisberg SP, McCann D, Desai M, Rosenbaum M, Leibel RL, Ferrante AW Jr. Obesity is associated with macrophage accumulation in adipose tissue. *J Clin Invest*. 2003;112:1796–1808. doi: 10.1172/JCI200319246
  33. Bugianesi E, Pagotto U, Manini R, Vanni E, Gastaldelli A, de lasio R, Gentilcore E, Natale S, Cassader M, Rizzetto M, et al. Plasma adiponectin in nonalcoholic fatty liver is related to hepatic insulin resistance and hepatic fat content, not to liver disease severity. *J Clin Endocrinol Metab*. 2005;90:3498–3504. doi: 10.1210/jc.2004-2240
  34. Huang XD, Fan Y, Zhang H, Wang P, Yuan JP, Li MJ, Zhan XY. Serum leptin and soluble leptin receptor in non-alcoholic fatty liver disease. *World J Gastroenterol*. 2008;14:2888–2893. doi: 10.3748/wjg.14.2888
  35. Zhang M, Lin J, Wang S, Cheng Z, Hu J, Wang T, Man W, Yin T, Guo W, Gao E, et al. Melatonin protects against diabetic cardiomyopathy through Mst1/Sirt3 signaling. *J Pineal Res*. 2017;63. doi: 10.1111/jpi.12418
  36. Devereux RB, Roman MJ, Paranicas M, O'Grady MJ, Lee ET, Welty TK, Fabsitz RR, Robbins D, Rhoades ER, Howard BV. Impact of diabetes on cardiac structure and function: the strong heart study. *Circulation*. 2000;101:2271–2276. doi: 10.1161/01.CIR.101.19.2271
  37. Lee M, Gardin JM, Lynch JC, Smith VE, Tracy RP, Savage PJ, Szklo M, Ward BJ. Diabetes mellitus and echocardiographic left ventricular function in free-living elderly men and women: the cardiovascular health study. *Am Heart J*. 1997;133:36–43. doi: 10.1016/S0002-8703(97)70245-X
  38. Al-Rasheed NM, Al-Rasheed NM, Hasan IH, Al-Amin MA, Al-Ajmi HN, Mohamad RA, Mahmoud AM. Simvastatin ameliorates diabetic cardiomyopathy by attenuating oxidative stress and inflammation in rats. *Oxid Med Cell Longev*. 2017;2017:1092015. doi: 10.1155/2017/1092015
  39. McGavock JM, Lingvay I, Zib I, Tillery T, Salas N, Unger R, Levine BD, Raskin P, Victor RG, Szczepaniak LS. Cardiac steatosis in diabetes mellitus: a 1h-magnetic resonance spectroscopy study. *Circulation*. 2007;116:1170–1175. doi: 10.1161/CIRCULATIONAHA.106.645614
  40. Sharma S, Adrogue JV, Golfman L, Uray I, Lemm J, Youker K, Noon GP, Frazier OH, Taegtmeier H. Intramyocardial lipid accumulation in the failing human heart resembles the lipotoxic rat heart. *FASEB J*. 2004;18:1692–1700. doi: 10.1096/fj.04-2263com
  41. Zlobine I, Gopal K, Ussher JR. Lipotoxicity in obesity and diabetes-related cardiac dysfunction. *Biochim Biophys Acta*. 2016;1861:1555–1568. doi: 10.1016/j.bbali.2016.02.011
  42. Sletten AC, Peterson LR, Schaffer JE. Manifestations and mechanisms of myocardial lipotoxicity in obesity. *J Intern Med*. 2018;284:478–491. doi: 10.1111/joim.12728
  43. Puliniilkunnil T, Kienesberger PC, Nagendran J, Waller TJ, Young ME, Kershaw EE, Korbutt G, Haemmerle G, Zechner R, Dyck JR. Myocardial adipose triglyceride lipase overexpression protects diabetic mice from the development of lipotoxic cardiomyopathy. *Diabetes*. 2013;62:1464–1477. doi: 10.2337/db12-0927
  44. Haemmerle G, Moustafa T, Woelkart G, Buttner S, Schmidt A, van de Weijer T, Hesselink M, Jaeger D, Kienesberger PC, Zierler K, et al. Atgl-mediated fat catabolism regulates cardiac mitochondrial function via PPAR-alpha and PGC-1. *Nat Med*. 2011;17:1076–1085. doi: 10.1038/nm.2439
  45. Anderson EJ, Kypson AP, Rodriguez E, Anderson CA, Lehr EJ, Neuffer PD. Substrate-specific derangements in mitochondrial metabolism and redox balance in the atrium of the type 2 diabetic human heart. *J Am Coll Cardiol*. 2009;54:1891–1898. doi: 10.1016/j.jacc.2009.07.031
  46. Anderson EJ, Rodriguez E, Anderson CA, Thayne K, Chitwood WR, Kypson AP. Increased propensity for cell death in diabetic human heart is mediated by mitochondrial-dependent pathways. *Am J Physiol Heart Circ Physiol*. 2011;300:H118–124. doi: 10.1152/ajpheart.00932.2010
  47. Shen X, Zheng S, Metreveli NS, Epstein PN. Protection of cardiac mitochondria by overexpression of MnSOD reduces diabetic cardiomyopathy. *Diabetes*. 2006;55:798–805. doi: 10.2337/diabetes.55.03.06.db05-1039
  48. Tong M, Saito T, Zhai P, Oka SI, Mizushima W, Nakamura M, Ikeda S, Shirakabe A, Sadoshima J. Mitophagy is essential for maintaining cardiac function during high fat diet-induced diabetic cardiomyopathy. *Circ Res*. 2019;124:1360–1371. doi: 10.1161/CIRCRESAHA.118.314607
  49. Hsieh CC, Li CY, Hsu CH, Chen HL, Chen YH, Liu YP, Liu YR, Kuo HF, Liu PL. Mitochondrial protection by simvastatin against angiotensin II-mediated heart failure. *Br J Pharmacol*. 2019;176:3791–3804. doi: 10.1111/bph.14781
  50. Makino A, Scott BT, Dillmann WH. Mitochondrial fragmentation and superoxide anion production in coronary endothelial cells from a mouse model of type 1 diabetes. *Diabetologia*. 2010;53:1783–1794. doi: 10.1007/s00125-010-1770-4

- 
51. Montaigne D, Marechal X, Baccouch R, Modine T, Preau S, Zannis K, Marchetti P, Lancel S, Neviere R. Stabilization of mitochondrial membrane potential prevents doxorubicin-induced cardiotoxicity in isolated rat heart. *Toxicol Appl Pharmacol*. 2010;244:300–307. doi: 10.1016/j.taap.2010.01.006
  52. Marin-Garcia J, Akhmedov AT. Mitochondrial dynamics and cell death in heart failure. *Heart Fail Rev*. 2016;21:123–136. doi: 10.1007/s10741-016-9530-2
  53. Feldstein AE, Werneburg NW, Canbay A, Guicciardi ME, Bronk SF, Rydzewski R, Burgart LJ, Gores GJ. Free fatty acids promote hepatic lipotoxicity by stimulating TNF- $\alpha$  expression via a lysosomal pathway. *Hepatology*. 2004;40:185–194. doi: 10.1002/hep.20283
  54. Eitel K, Staiger H, Brendel MD, Brandhorst D, Bretzel RG, Haring HU, Kellerer M. Different role of saturated and unsaturated fatty acids in beta-cell apoptosis. *Biochem Biophys Res Commun*. 2002;299:853–856. doi: 10.1016/S0006-291X(02)02752-3
  55. Gomes LC, Di Benedetto G, Scorrano L. During autophagy mitochondria elongate, are spared from degradation and sustain cell viability. *Nat Cell Biol*. 2011;13:589–598. doi: 10.1038/ncb2220

# **Supplemental Material**

**Table S1.** Primer sequences used in this research.

<b>Gene Name</b>	<b>Forward Primer</b>	<b>Reverse Primer</b>
18s	GTAACCCGTTGAACCCCAT	CCATCCAATCGGTAGTAGCG
Sdha	GGAACACTCCAAAAACAGACCT	CCACCACTGGGTATTGAGTAGAA
ATP5j	TATTGGCCCAGAGTATCAGCA	GGGGTTTGTCGATGACTTCAAAT
ATP5h	GCTGGGCGTAAACTTGCTCTA	CAGACAGACTAGCCAACCTGG
Drp1	CAGGAATTGTTACGGTTCCTAA	CCTGAATTA ACTTGTCCTCGTA
Sirt1	GCTGACGACTTCGACGACG	TCGGTCAACAGGAGGTTGTCT
Mfn2	ACCCCGTTACCACAGAAGAAC	AAAGCCACTTTCATGTGCCTC
Mfn1	ATGGCAGAAACGGTATCTCCA	CTCGGATGCTATTCGATCAAGTT
SOD	AACCAGTTGTGTTGTCAGGAC	CCACCATGTTTCTTAGAGTGAGG
GST	ATGCCACCATACACCATTGTC	GGGAGCTGCCCATACAGAC
NQO1	AGGATGGGAGGTA CT CGAATC	AGGCGTCCTTCCTTATATGCTA
KEAP1	TGCCCTGTGGTCAAAGTG	GGTTCGGTTACCGTCCTGC
NRF2	TCTTGAGTAAGTCGAGAAGTGT	GTTGAAACTGAGCGAAAAAGGC

NRF1	TATGGCGGAAGTAATGAAAGACG	CAACGTAAGCTCTGCCTTGTT
PPAR $\alpha$	AGAGCCCCATCTGTCCTCTC	ACTGGTAGTCTGCAAAACCAAA
PGC1 $\alpha$	AAGTGGTGTAGCGACCAATCG	AATGAGGGCAATCCGTCTTCA
PDK4	AGGGAGGTCGAGCTGTTCTC	GGAGTGTTCACTAAGCGGTCA
CD36	ATGCCGGTTGGAGACCTACTCA	GCTATTCTTTGCCACTTCCTCTGG
GLUT4	CTCATGGGCCTAGCCAATGC	CCCTGATGTTAGCCCTGAGTA
DGAT1	GTGCCATCGTCTGCAAGATTC	GCATCACCACACACCAATTCAG
PNPLA2	GGATGGCGGCATTTTCAGACA	CAAAGGGTTGGGTTGGTTCAG
ACAA2	ATGTGCGCTTCGGAACCAAA	CAAGGCGTATCTGTCACAGTC
MLYCD	GCACGTCCGGGAAATGAAC	GCCTCACACTCGCTGATCTT
ACADM	GAGGCTACAAGGTCCTGAGAA	GGGTATTCCCGCTTTTATCG
PDHA	GAAATGTGACCTTCATCGGCT	TGATCCGCCTTTAGCTCCATC
HK2	CTAAGGGGTTCAAGTCCAGTGG	AGACCAATCTCGCAGTTCTGA

---